UNIVERSITÀ DEGLI STUDI DI SALERNO

DIFARMA

UNIVERSITÀ DEGLI STUDI DI SALERNO

Dipartimento di Farmacia

PhD program in

Drug Discovery and Development

XXXV Cycle – Academic Year 2022-2023

PhD thesis in:

Effects of natural iron chelators on dendritic cells: anti-inflammatory activity, phenotypic characterization, and metabolomic analysis

Candidate:
Dott. *Giulio Verna*

Supervisor:
Chiar.mo Prof. *Pietro Campiglia*

Co-supervisor:
Chiar.mo Prof. *Stefania Marzocco*

Coordinator: Chiar.mo Prof. *Gianluca Sbardella*

1. Abstract

Dendritic cells (DCs) are key regulators of the immune system that patrol all the compartments of the body. When exposed to danger signals, DCs mature, migrate to the draining lymph nodes, and activate the adaptive immune response. Significant differences exist between immature DCs (iDCs) and mature DCs (mDCs), the first guard the host periphery and support homeostasis, and the second present antigens and support inflammation. Bacteria are among the most common maturational stimuli that cause the switch from iDCs to mDCs.

DCs can also be divided by lineage into myeloid dendritic cells (mDCs) and plasmacytoid dendritic cells (pDCs). They are both present in mucosal tissues and regulate the immune response by secreting chemokines and cytokines.

Several key elements play an important role in this process, among those, intracellular iron is an underinvestigated player required to initiate and sustain their inflammatory response. It has been recently demonstrated that the exposure of DCs to naturally derived iron chelators (mainly polyphenols or flavonoids like quercetin) reduce the intracellular iron pool and, consequently, prevents DCs' secretion of inflammatory cytokines and antigen-presenting abilities.

Iron content in the body is finely regulated, but several pathologies, as well as diet, may affect its level. Little is known about the effects of DCs maturation in iron overload conditions or iron-deprived conditions. The aim of the PhD work will be the investigation of the metabolic pathways characterizing DCs in resting and active conditions and identify the potential protective effects of nutritional-derived biochelators in a murine model of chronic intestinal inflammation.

This research work can be divided into three phases: the first consisted of the study of the role of iron in the maturational process of DCs, the second analyzed the metabolomic profile of active and inactivated DCs while the third involved the use of a mouse model of chronic colitis to study the effects of polyphenols *in vivo*.

The results clearly describe the role of iron in the maturational process of DCs as cells cultured in an iron-enriched culture medium for ten days failed to differentiate into conventional $CD11c^{+}MHCII^{hi}$ DCs and respond to LPS (Lipopolysaccharides). Phenotypically, these cells appeared smaller than control DCs but vital and able to perform FITC-dextran (Fluorescein isothiocyanate-dextran) endocytosis. At the molecular level, cells cultured in iron-enriched conditions showed increased *Arg1* while decreased *Pu.1* and *Irf8* expression.

DCs activation is linked to metabolic changes that are essential to support their activity and function. Hence, targeting DCs metabolism represents an opportunity to modify the inflammatory and immune response. Using untargeted metabolomics, it was possible to evaluate the modulation of mDCs metabolism after stimulation with LPS and assess polyphenol effects. Both fraction C derived from *Humulus lupulus* and quercetin reduced the production of several inflammatory cytokines, but differently from quercetin, the fraction C mechanism was independent of extracellular iron and showed a different metabolic pathway. The analysis revealed a modulation of several key pathways linked to pro-inflammatory activity and glycolysis.

The last part of the work studied the effects of anthocyanins derived from *B1 Pl1* purple corn cobs through ethanol extraction on a mouse model of chronic colitis: the SAMP1/YitFc. These mice develop spontaneous ileitis that resembles human Crohn's disease with a typical discontinuous pattern. After 70 days of anthocyanin intervention, we observed positive changes in the histology score and microbial populations.

2. Introduction

2.01. Dendritic cells

Dendritic cells (DCs) are antigen-presenting cells able to capture, process, and present non-self-antigens to initiate and support the adaptive immune response [1,2]. They are the important link between innate and adaptative immunity; they sense antigens through their membrane toll-like receptors (TLRs) [3] and intracellular Nucleotide-binding oligomerization domain-containing 2 (NOD)-like receptors [4], thus they degrade them to small peptides that get presented to effector cells using the MHCII complex [5]. They also express costimulatory molecules like CD80 and CD86 that form the antigen-presenting complex with T cells. In addition, they secrete a different number of cytokines and chemokines to direct and orchestrate the immune system.

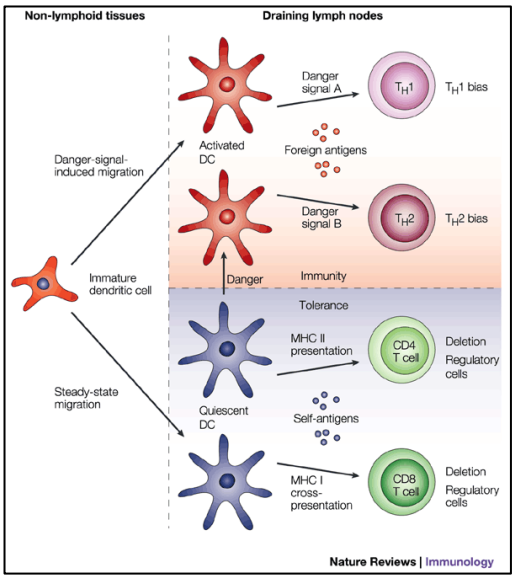

Figure 1. Dendritic cell response after activation

DCs originate from common progenitors, and differentiate in peripheral tissues; their major role consists of presenting microbial antigens to T lymphocytes to initiate a powerful immune response [6]. Immature DCs can perform pinocytosis and phagocytosis but cannot present the sampled antigens to other cells, they are also inefficient at secreting cytokines. The encounter with an antigen that binds to the TLRs turns on the maturation mechanism and activates antigen presentation and cytokine secretion; DCs increase the production and expression of MHCII complexes, while they migrate to lymph nodes and T cell-rich organs where they stimulate antigen-specific T-naïve cells. Depending on their stimuli, they are capable of driving the immune response towards a tolerogenic or pro-inflammatory outcome

[7]; they can select the best immune response to direct towards a specific antigen, thus activating the most effective T cell subtype. Moreover, DCs can mature and be present at a steady state where they present self-antigens to activate Treg cells [8,9].

2.02. Plasmacytoid dendritic cells

DCs can be divided into many subsets according to membrane proteins and their transcriptome [10]. This includes genes associated with pathogen sensing and induction of type-I interferons (*Irf7*, *Tlr7*, *Slc15a4*, and *Pacsin1*), secretion (*Derl3*, *Lamp5*, and *Scamp5*), and the plasmacytoid dendritic cell (pDCs) master regulator transcription factor *Tcf4*, along with its binding targets (*Sla2*, *Ptcra*, *Ptprcap*). In contrast, myeloid DCs (mDCs) express markers like *Cd2*, *Cx33cr1*, *Cd33/Siglec3*, *Cd5*, and *Siglec1/Cd169* [11]. Also, the two populations of DCs can be distinguished mDCs and pDCs by lineage derivation [12]. pDC differentiation is driven by FMS-like tyrosine kinase 3 ligand (Flt3L) [13], while PU.1 (also known as SPI1) differentiates progenitors from mDCs [14]. mDCs also express more *Irf8* than pDCs [15]. pDCs can be distinguished from mDCs by some specific membrane markers. Murine pDCs express less CD11c but, differently from mDCs, they are positive to B220 and Ly6C, thus appearing $CD11c^{int}B220^{+}Ly6C^{+}$ compared to mDCs that are $CD11c^{high}B220^{-}Ly6C^{-}$ [16,17]. Moreover, pDCs express fewer MHCII molecules than their myeloid counterparts [17].

pDCs are less frequent than any other DC subtype, they are mainly present in blood and lymphoid organs; they express fewer pattern recognition receptors (PRR) like TLR7 and TLR9 to recognize foreign nucleic acids and secrete type-I interferons (IFNα, IFNβ) [18].

2.03. Iron and immune cells

Iron is a necessary microelement for humans and animals, its excess and lack can have severe effects on health and disease. Iron is crucial for immune cell activation as its intracellular uptake is required for inflammatory phenotype development while extracellular secretion favors tolerance and tissue repair. Iron depletion from the

culture medium reduces immune cell inflammatory abilities; *vice versa*, growth in elevated iron concentrations results in macrophage polarization into M1 type [19,20].

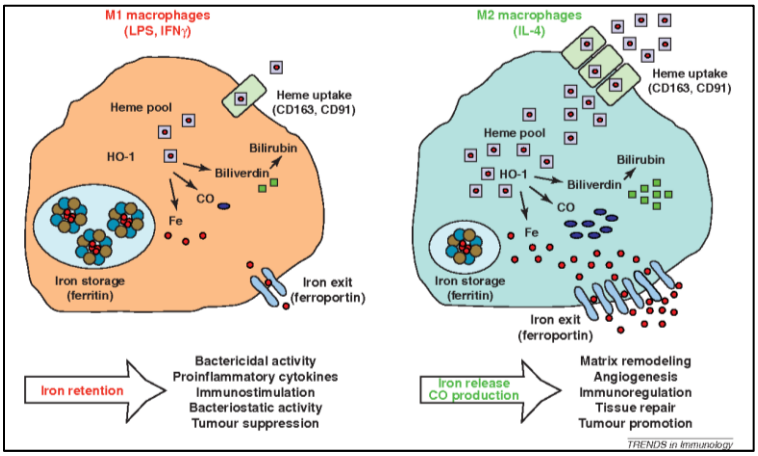

Figure 2. Macrophage iron metabolism

A study conducted on Taiwanese patients affected by iron deficiency anemia and relative controls showed a trend towards an increased risk of contracting tuberculosis for anemic patients versus healthy controls, with a higher risk in younger patients compared to older ones [21].

Deferoxamine (DFO) induced the downregulation of MHCI in human melanoma cells and on primary macrophages, this iron-chelating mechanism promoted ferritin reduction and subsequently intracellular iron accumulation. Sottile et al. discovered that DFO treatment impairs the synthesis of MHCI induced by inflammatory cytokines [22]. Melanoma cells became more sensitive to NK cell killing in the presence of DFO in the medium, this is due to the downregulation of MHCI on tumor cells that allow natural killer cells to attack. It is also plausible that iron concentration may modulate NK cell activity and that low ferritin and low MHCI can activate NK cells to secrete more pro-inflammatory cytokines [23-25].

A hydroferrate fluid named MRN-100 containing ferrous and ferric iron as well as plant extracts had many protective effects against oxidative stress and chemical carcinogenesis [26,27]. DCs treated with MRN-100 showed an increase in the expression of surface activation markers CD80 and CD86; they also expressed high

levels of IL-10. LPS treatment did not change cytokine secretion amounts for IL-6 and TNF but improved the release of IL-10. CD4 cells cocultured with MRN-100 pretreated DCs showed comparable levels of cytokines secretion, though lower levels of TNF were released when compared to CD4 cells primed by untreated DCs [28].

Iron chelation by quercetin, indeed, modulated the production of NOS by rat macrophages in an animal model of iron-deficient anemia; moreover, when iron supplementation was provided, quercetin reduced its absorption with no effect on anemia-related symptoms [29].

A study performed in Egypt on IDA children provided important insights into the importance of iron in the secretion of various inflammatory cytokines, mainly IL-6 and IL-8; a marked reduction in antibody production and in phagocytic activity compared to control children was also observed [30].

Rahmani investigated Algerian children with anemia and obtained similar results as an Egyptian study. Anemic children produced fewer antibodies and also had significantly decreased monocyte and neutrophil counts compared to healthy children [31].

Supernatants from LPS-treated macrophages have smaller iron concentrations compared to IL-10-treated macrophages, indicating a difference in iron metabolism between M1 and M2 cells. The M2 cells release iron in their environment and stimulate cell survival, while M1 macrophages sequester iron and can inhibit tumor cell growth. Using an intracellular iron chelator (administered as a prochelator), it was seen that the iron concentration in the supernatants of M2 cells was lowered, as those cells switched their phenotype to M1 macrophages and reverted their tumor-enhancing profile [32].

Turkish pediatric studies focused on iron-deficient children showed a decreased percentage of oxidative stimulated neutrophils as well as phagocytic ones compared

to healthy controls; nevertheless, the neutrophil to lymphocyte ratio was increased probably due to a reduced lymphocyte population [33].

Iron concentrations have effects on all types of immune cells. Peripheral blood lymphocytes sampled from IDA patients were altered in the percentage of CD8, plus a reduction in cytokine secretion crucial for lymphocyte maturation was observed. Iron therapy proved to help compensate the imbalanced lymphocyte populations and increased their maturation profiles [24,25].

In a murine model of iron deficiency, Jiang et al showed impairment in the proliferation of B cells. Their results indicated an important role of iron in the regulation of two cyclins necessary for the division of T and mainly B cells, preventing their aggregation in the germinal center of lymph nodes and the subsequent events that characterize B cells' clonal selection [34].

Another study performed on iron-deficient anemic children confirmed the alteration in lymphocytic populations with a marked reduction in the $CD4^+$ cells and a great increase in $CD8^+$ cells. Interestingly, this trend was also observed in children with latent anemia, thus indicating the importance of early diagnosis [35].

Low body iron at birth potentially increases the risk of allergies [36]; similarly decreased serum ferritin concentrations were found in children affected by atopic eczema [37]. Clinical studies like these indicate that allergic patients often have low iron storage and a consequent dysregulated immune system. T-helper cells are influenced in different ways by iron, the lack of the metal alters more markedly Th1 cells and their proliferation rates while Th2 cells are less affected by iron shortage as they can keep their intracellular iron pools mostly untouched. As consequence, Th2 cells will develop and establish, with their peculiar cytokine production and IgE induction, the conditions that allow allergic sensitization to happen [38].

IFNγ and GM-CSF, two crucial cytokines [39,40], are finely regulated by iron. Deferoxamine showed efficient suppression of Th cells; this effect was lost if excess iron was added to the culture medium [41].

2.04. Polyphenols

Polyphenols are bioactive phytochemicals that can be divided into subclasses such as flavonoids, stilbenes, phenolic acids, and lignans. Flavonoids are the most represented and can be further divided into flavan-3-ols, flavonols, flavones, isoflavones, flavanones, and anthocyanins. They are present in nature in glycoside and non-glycosylated form, this can influence their bioavailability and metabolism. Normally they are absorbed in the small intestine, but they can also be metabolized by colonic bacteria; in both cases, they can influence immune cells to a different extent [42].

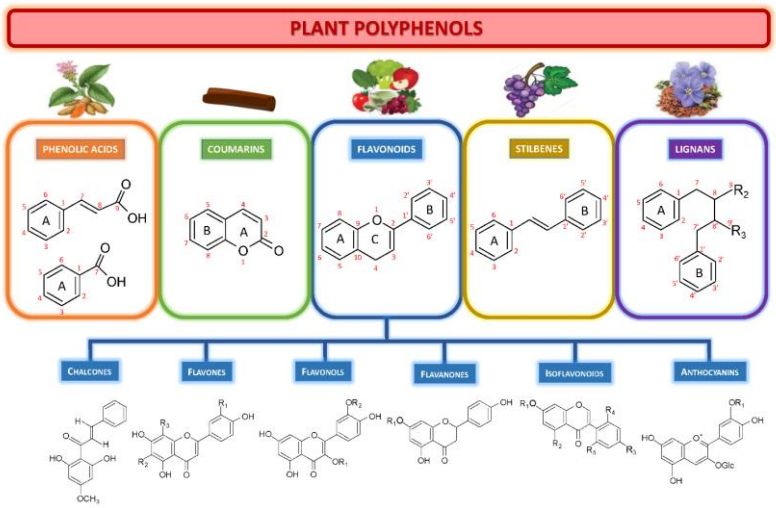

Figure 3. Different polyphenol classes and their structure

Polyphenols are natural iron chelators found in a great variety of fruits and vegetables and can be used to reduce inflammatory cytokine secretion, a peculiar characteristic that is lost when immune cells are grown in excess of iron [43]. Indeed, the anti-inflammatory abilities of polyphenols depend on their iron chelating abilities that promote DCs iron export in the culture media and, thus, cytoplasmic depletion of the iron reservoir [19,44,45]. Recent studies investigated the effects of many polyphenols extracted from vegetables like lettuce and orange on macrophages, showing a reduction in the secretion of inflammatory cytokines [46-48].

The maturation of DCs is characterized by great metabolic switches [49,50], and since iron is abundant in inflammatory conditions, DCs cultured in excess or deprived of iron represent a good model to identify metabolic products involved in dysregulated inflammation.

In healthy conditions, transferrin saturation is approximately 30%, but when circulating iron saturates transferrin's binding capacity, non–transferrin-bound iron (NTBI) is produced [51].

Ineffective hematopoiesis leading to peripheral blood cytopenia is often caused by myeloid malignancies like myelodysplastic syndrome (MDS) [52] but also by different forms of anemia and β-thalassemia. Patients affected by anemia become transfusion dependent, but due to the combination of ineffective hematopoiesis and repeated blood transfusions, they are often subject to iron overload that promotes iron-induced toxicity due to the production of reactive oxygen species (ROS) [53,54]. Iron excess can be deposited in the liver, heart, spleen, pancreas, bone marrow, and other tissues, resulting in tissue damage and fibrosis [55,56]. Jin et al. recently demonstrated that iron overload impairs erythroid maturation in a model of MDS mice [57].

Polyphenols and their metabolites influence intestinal microbiota and shape its population in a way that inflammation can be reduced. Several pieces of evidence proved the benefits of polyphenol administration to human patients and murine models of chronic colitis [44,50,58-64]. Bronze tomatoes can reduce the inflammation in the Winnie model of ulcerative colitis (UC) [65], favoring the growth of beneficial bacteria [66,67]; moreover, they had positive effects on lactation and mother-to-litter microbial transfer [68]. The same can be said of Bronze tomato effects on DCs where it decreased the inflammatory cytokine secretion while increasing anti-inflammatory IL-10 production [69].

While many studies focused on cytokine secretion and molecular pathways, the ability of natural compounds to modulate the metabolic pathways that regulate the function of immune cells has also been indeed scarcely investigated.

2.05. Inflammatory bowel diseases

Inflammatory bowel diseases (IBDs) are gastrointestinal disorders driven by a dysregulated immune response and strong dysbiosis, that lead to chronic and relapsing diseases [70]. Environment and genetic predisposition are also key factors to the pathogenesis that can manifest as UC or Crohn's disease (CD) based on the location of the inflammation. Several cytokines were reported to have a key role in dysregulated response that is ongoing in IBD patients, tumor necrosis factor (TNF) is one of them. Nowadays most state-of-the-art therapies are directed against it [71]. UC affects only the colon with continuous lesions which can lead to erosions, ulcers, and bloody diarrhea. CD is progressive and destructive; it can affect all the gastrointestinal tract from mouth to anus. Furthermore, half of all patients develop intestinal complications, such as strictures or fistulae.

Diet has an important effect on microbial composition. In two prospective studies in Sweden, greater adherence to a Mediterranean diet was associated with a substantially lower risk of later-onset CD [72].

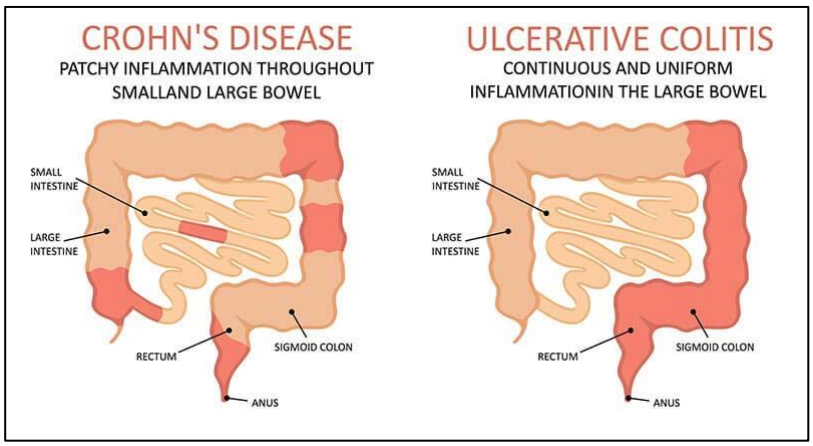

Figure 4. The two different types of IBD

Genetic predisposition is often associated with mutations in about 200 loci [73]; most of them are related to a low risk while other variants in genes like NOD2 or IL-23 can have a major impact on disease onset. CD arises from excessive T helper 1 (Th1) and Th17 cell responses, in turn, Th1 and Th17 cells secrete the proinflammatory cytokines IL-17, IFNγ, and TNF, which further boost inflammation acting on other cells [74].

Conventional therapies include corticosteroids and biological agents that have shown efficacy in maintenance therapy. Anti-TNF therapies (such as infliximab, adalimumab, and certolizumab) have revolutionized the treatment of CD in the past two decades. These agents have become increasingly widespread and commonly used, however, they can present several drawbacks like the production of anti-antibodies by the patient that becomes unable to respond to the therapy [75-77].

2.06. Dendritic cells in IBD

Recently, there have been observed aberrant numbers of DCs in CD patients; pDCs were less present while mDCs were more active and secreted more cytokines [78].

DCs that express CD-associated variants are defective in [79,80] the IL-23 axis [81,82]. Dysfunctional LP DCs produce IL-12/23p40 and IL-6 more than IL-10 compared to healthy controls [12]. Production of pro-inflammatory cytokines by colonic DCs in CD correlates with disease activity [83,84].

$CD103^+$ DCs have been considered tolerogenic in mice [85,86], which are believed to be important in initiating T-cell responses including induction of $FOXP3^+$ regulatory Tregs [86]; this subset of DCs is often aberrant in CD patients [87].

2.07. SAMP1/YitFC mouse model

This line of mice was generated from the ARK/J strain through selective breeding at the University of Kyoto. After an accidental cross with a non-ARK/J strain, some litters expressed an accelerated senescent phenotype. This senescence-accelerated mice-prone (SAMP) model was then bred for 20 generations until it developed spontaneous ileitis and lost the senescent phenotype. The new strain SAMP1/Yit

developed chronic intestinal inflammation, mainly localized in the ileum with a discontinuous pattern and immune cell infiltrate. The SAMP1/Yit mice were later transferred to the University of Virginia where they also developed perianal fistulae with a 5 to 10% of penetrance, high interferon γ (IFN-γ) production, and increased fibrosis; moreover, in these mice an early onset of colitis (starting at 10 weeks of age) was observed, thus naming this new strain SAMP1/YitFC (hereafter referred as SAMP).

Typical macroscopic and histological features of these mice are focal areas of necrosis and inflammation in the ileum with a cobblestone pattern, crypt elongation and immune cell infiltrate.

Immune phenotyping showed a marked involvement in the IL-17/IL-23 pathway with Th17 cells that were predominantly present in the mucosa as well as IL-33 downstream production [88,89].

Even though SAMP mice do not harbor mutations in the NOD2 gene they present an impaired response to its activation with dysregulated cytokine secretion and failure to clear bacterial infections. This is in line with what is observed in CD patients that, despite being wild-type (WT) for NOD2, show a dysregulated immune response dependent on this gene [90].

Recently, another important mutation was discovered in SAMP mice, they do not express CCL21 and this results in a defective migration of DCs from the periphery to the mesenteric lymph node (MLN). In young mice, before the onset of chronic inflammation, there is already a reduction in the expression of CCL21 and DCs fail to activate Treg cells in the MLN after they get activated in the terminal ileum. Moreover, SAMP DCs' hyporesponsiveness to retinoic acid further decreased their ability to induce Treg activation and their subsequent control of intestinal inflammation [91].

3. Experimental plan

The main objective of the PhD project is to observe the effects of polyphenols on DCs and chronic colitis through molecular and metabolomics approaches.

Primary DCs will be harvested and differentiated from WT murine bone marrow progenitors using the established culture method with GM-CSF and IL-4 [92,93]. Mature cells will be stimulated with LPS and polyphenols of choice, in normal conditions or iron-enriched culture medium; cells will also be used for RNA extraction and metabolomic analysis while supernatants will be used for the quantification of secreted cytokines. pDCs will be cultured with Flt3L and processed in the same manner as mDCs [94].

The phenotype of DCs will be assessed by cytofluorimetry with the superficial markers CD11b, CD11c, F4/80, CD80, CD86, Ly6G, B220, and MHCII [17,94].

Their metabolome will be analyzed with a combined approach of liquid chromatography and mass spectrometry (UHPLC-MS) [95] to evaluate the metabolic differences between DCs grown in conventional conditions and with iron excess and the polyphenol effects.

Lastly, the obtained results are going to be translated to an *in vivo* chronic inflammation model (SAMP model) testing purple corn anthocyanins [96,97] effects on a CD-like disease model. At the end of the experiment metagenomic and metabolomic analysis will be performed.

4. Materials and methods

4.01. Animal studies

Our investigations were performed under the relevant animal protocols, which were approved by the Institutional Animal Care Committee of the National Institute of Gastroenterology "S. de Bellis" (Organism engaged for compliance of Animal Wellbeing: OPBA) and The Institutional Animal Care and Use Committee (IACUC) protocol 2014-0158. All of the animal experiments were carried out according to the national guidelines of Italian Directive n. 26/2014 and approved by the Italian Animal Ethics Committee of the Ministry of Health—General Directorate of Animal Health and Veterinary Drugs (DGSA Prot. 768/2015-PR 27/07/2015). All animals were maintained in a controlled environment (20–22° C, 12 h light and 12 h dark cycles, and 45–55% relative humidity).

4.02. Generation and culture of murine DCs

mDCs and pDCs were obtained from wild-type mice purchased from Jackson Laboratories: (C57BL/6, Stock No.: 000664). Six- to eight-week-old mice were sacrificed, and their tibiae and femurs were flushed with 0.5 mM EDTA (Thermo Fisher Scientific, MA, USA). Red blood cells were lysed with an ACK buffer (Thermo Fisher Scientific, MA, USA).

For mDCs generation, the single cell suspension was plated in 10 mL dishes at the concentration of $1x10^6$ cells/mL for 10 days in RPMI 1640 medium (Thermo Fisher Scientific, MA, USA) supplemented with 10% heat-inactivated fetal bovine serum (FBS, Thermo Fisher Scientific, MA, USA), 100 U/mL penicillin/streptomycin (Thermo Fisher Scientific, MA, USA), 1% HEPES 1M (Thermo Fisher Scientific, Waltham, MA, USA), 1% non-essential aminoacids 100 mM (Thermo Fisher Scientific, Waltham, MA, USA), 1% sodium pyruvate 100 mM (Thermo Fisher Scientific, Waltham, MA, USA) 25 ng/mL mGM-CSF (Miltenyi Biotec, Bergisch Gladbach, Germany), 25 ng/mL mIL-4 (Miltenyi Biotec, Bergisch Gladbach, Germany) as previously done, and cultured at 37 °C in a humidified 5% CO^2 atmosphere.

Cells grown in an iron-enriched medium were cultured in the same conditions but 10% heat-inactivated iron-enriched fetal bovine serum (Thermo Fisher Scientific, MA, USA) was used instead of normal serum.

For pDCs generation, cells were plated in a 6-well culture plate at the concentration of $2x10^6$ cells/mL in the same culture medium as mDCs with 200 ng/mL mFlt3L (Miltenyi Biotec, Bergisch Gladbach, Germany) instead of mGM-CSF and mIL-4 and cultured at 37°C in a humidified 5% CO_2 atmosphere.

For the coculture experiments, mDCs and pDCs were harvested from their respective culture plates on day 10 after isolation and plated in a 1:1 ratio in RPMI 1640 medium (Thermo Fisher Scientific, Waltham, MA, USA) supplemented with 10% heat-inactivated FBS (Thermo Fisher Scientific, Waltham, MA, USA), 100 U/mL penicillin/streptomycin (Thermo Fisher Scientific, Waltham, MA, USA), 1% HEPES 1M (Thermo Fisher Scientific, Waltham, MA, USA), 1% non-essential aminoacids 100 mM (Thermo Fisher Scientific, Waltham, MA, USA), 1% sodium pyruvate 100 mM (Thermo Fisher Scientific, Waltham, MA, USA).

Mature mDCs and pDCs, after 10 days of culture were gently harvested and plated on a 6-well culture plate at the concentration of $3x10^6$ cells/mL for metabolomics, $1x10^6$ cells/mL for cytokine and RNA analysis and $2.5x10^6$ cells/mL for cytofluorimetry. Then, 25 µM of quercetin or one of the six concentrations (250 µg/mL, 125 µg/mL, 25 µg/mL, 12.5 µg/mL and 6.25 µg/mL) of Hop A, B, or C fraction was administered to the culture medium and, 24 h later, DCs and/or pDCs were stimulated with 1 µg/mL of Salmonella Typhimurium LPS (Sigma-Aldrich, St Louis, MO, USA). For the experiments that included iron treatment, quercetin or Hop C fraction was administered alone or in combination with 2 µM $FeCl_3$ (Sigma-Aldrich, St Louis, MO, USA) and 0.1 mM ascorbic acid (Sigma-Aldrich, St Louis, MO, USA).

pDCs and mDCs were also stimulated with 3 µg/mL CpG ODN 2216 or 3 µg/mL CpG ODN 2243 Control (Miltenyi Biotec, Bergisch Gladbach, Germany).

4.03. Enzyme-Linked Immunosorbent Assay (ELISA)

Cell supernatants were harvested 24 h after LPS or CpG stimulation and stored at -80°C until the analysis. They were tested for IL-12/23p40, IL-12p70, IL-10, IL-6, TNF, IL-1β, and IL-1α release in duplicate for three consecutive and independent experiments, using ELISA kits (RD Systems, Minneapolis, MN, USA) following the manufacturer's instructions. The same supernatants were also used for a multiplex cytokine assay with the Cytokine & Chemokine Convenience 36-Plex Mouse ProcartaPlex™ Panel 1A (Thermo Fisher Scientific, Waltham, MA, USA) following the manufacturer's instructions.

4.04. RNA extraction and qPCR analysis

Total RNA was isolated from all cells after 6 h post LPS stimulation using TRIzol® (Thermo Fisher Scientific, MA, USA), according to the manufacturer's instructions. Total RNA (1 μg) was reverse transcribed using the iScript cDNA Synthesis kit (Biorad, CA, USA) with random primers for cDNA synthesis. Gene expression was assessed using the following Taqman® probes: *Gapdh* Mm99999915_g1, *Pu.1/Spi1* Mm00488140_m1, *Irf8* Mm0042567_m1, *Tlr4* Mm00445273_m1, *Arg1* Mm00475988_m1, *Ap.1* Mm00495062_s1, *Ptger2* Mm00436051_m1, *Nrf2* Mm00477784_m1, *Irf7* Mm00516791_g1, *Ido2* Mm00524210_m1, *Hmox1* Mm00516005_m1, *Slpi* Mm00441530_g1, *Ifna2* Mm00833961_s1, *Ferroportin* Mm01254822_m1, *Nrf2* Mm00477784_m1, and *Nqo1* Mm00500821_m1 (all probes were bought from Thermo Fisher Scientific, Waltham, MA, USA).

Real-time analysis was performed on a CFX96 System (Biorad, CA, USA), and relative expression was calculated using the ΔΔCt method. At least three different experiments were performed.

4.05. Fluorescence microscopy

mDCs were cultured into 35 mm Glass Bottom Microwell Dishes (MatTek corporation, Ashland, MA, USA) and stimulated with LPS for 24 h. FITC-dextran MW 4000 (Sigma-Aldrich, St. Louis, MO, USA) was administered in the culture

dish for 2 h, before image acquisition. Cell nuclei were stained with DAPI (Thermo Fisher Scientific, MA, USA). Images were acquired with Leica DM6000B Microscope (Leica, Wetzlar, Germany).

4.06. Microscopy

mDCs were cultured into 35 mm Glass Bottom Microwell Dishes (MatTek corporation, Ashland, MA, USA) and stimulated with LPS for 24 h. Cells were fixed with two drops of PFA 4% (Sigma-Aldrich, St. Louis, MO, USA) for 2 min and then stained with two drops of hematoxylin (Diapath, Martinengo, Italy) for 4 min. The dishes were washed with dH2O and acquired with Leica DM6000B Microscope (Leica, Wetzlar, Germany).

4.07. Cytofluorimetric analysis

24 h after LPS stimulation, mDCs and pDCs were detached from the plates with PBS 1X (Gibco, MA, USA) + 0.5 mM EDTA (Thermo Fisher Scientific, MA, USA). Cells were then washed with PBS 1× + 0.5% bovine serum albumin (BSA, Sigma-Aldrich, St. Louis, MO, USA) and labeled with CD11b VioBrightFITC, MHCII PE, CD11c PECy5, F4/80 APC, CD80 FITC, CD86 FITC, CD8a FITC, Ly6C FITC, CD11c APC-Vio770, CD45R(B220) PE-Vio770, CD11c PE, MHCII APC, and 7-AAD PECy5 (all antibodies were acquired from Miltenyi Biotec, Bergisch Gladbach, Germany) for vitality staining. Flow Cytometer data analysis was performed using NAVIOS software (Beckman Coulter, Brea, CA, USA), with at least three experiments performed. Flow cytometer analysis was performed using Kaluza Software 1.5 (Beckman Coulter, Brea, CA, USA).

4.08. Cell isolation from mesenteric lymph nodes (MLN) and Peyer's patches (PP)

WT and Winnie mice were sacrificed, and their MLNs and PP were detached, cleaned from fat, and put in RPMI 1640 medium (Thermo Fisher Scientific, Waltham, MA, USA). To obtain a single-cell suspension, MLNs were smashed with PBS 1X (Thermo Fisher Scientific, Waltham, MA, USA) + 0.5 mM EDTA (Thermo

Fisher Scientific, Waltham, MA, USA) and passed through 40 µm cell strainers (Miltenyi Biotec, Bergisch Gladbach, Germany). The single-cell suspension from PP was obtained after digestion with collagenase type IV and DNase I (Sigma Aldrich, St. Louis, MO, USA) for 30 min at 37° C on a rocking platform. The resulting single-cell suspension was pelleted by centrifugation, washed with PBS 1X + 0.5 mM EDTA, and passed through 100 µm, 70 µm, and 30 µm cell strainers (Miltenyi Biotec, Bergisch Gladbach, Germany). Then, cell pellets were washed with PBS 1X + 0.5% bovine serum albumin (BSA, Sigma-Aldrich, St. Louis, MO, USA) and labeled for cytofluorimetric analysis.

4.09. Hop phytocomplex fractionation and characterization

The extraction, isolation, and characterization of the Hop fractions were performed by semi-preparative reversed liquid chromatography, as previously optimized, and the detailed parameters are reported in ESI.

4.10. Metabolomics sample preparation and analysis

mDCs were harvested after stimulation with PBS 1X (Gibco, MA, USA) + 0.5 mM EDTA (Thermo Fisher Scientific, Waltham, MA, USA) and pelleted, the solution was removed and the pellet was frozen at -80°C. Pelleted cells were thawed on ice and 100 µL of ice-cold MeOH/H2O (80:20 v/v) was added. The samples were extracted in an ultrasonic bath for 6 min, vortexed for 30 s, and finally centrifuged at 14 680 rpm, for 10 min at 4 °C. The supernatants were dried under nitrogen and were reconstituted in 100 µL of ACN/H2O (70:30) + 0.1% HCOOH (v/v) before HRMS analysis. A pooled quality control (QC) sample was prepared by pooling an aliquot of cellular extract from each sample. Unless otherwise described, all solvents and additives were LCMS grade and purchased by Merck (Darmstadt, Germany).

Analyses were performed on a Thermo Ultimate RS 3000 coupled online to a Q-Exactive hybrid quadrupole Orbitrap mass spectrometer (Thermo Fisher Scientific, Bremen, Germany) equipped with a heated electrospray ionization probe (HESI II). The MS was calibrated using Thermo Pierce™ calibration solutions in both

polarities. The analysis of cellular metabolites was performed in HILIC mode, with an Acquity BEH Amide (150 × 2.1 mm; 1.7 μm) protected with a VanGuard amide precolumn (5 × 2.1 mm; 1.7 μm) (Waters, Milford, MA, U.S.A). The column temperature was set at 45 °C, and the flow rate was 0.350 mL/min. The mobile phase was (A): 5 mM CH3COONH4 in H2O/ACN (95 : 5 v/v) + 0.1% CH3COOH (v/v) and (B): 5 mM CH3COONH4 in H2O/ACN (5 : 95 v/v) + 0.1% CH3COOH (v/v). The following gradient was employed: 0 min, 99%B, 0.01–1 min, 99%B, 1.01–12 min, 99.01–20%B, 12.01–13 min, 20%B, returning to 99% in 0.1 min, and 3 μL and 5 μL were injected for ESI+ and ESI− analysis, respectively. Full MS (80–800 m/z) and data-dependent MS/MS were performed at a resolution of 35.000 and 15 000 FWHM, respectively, and normalized collision energy (NCE) values of 10, 20, and 30 were used. Source parameters: sheath gas pressure, 50 arbitrary units; auxiliary gas flow, 13 arbitrary units; spray voltage, +3.5 kV, −2.8 kV; capillary temperature, 310 °C; and auxiliary gas heater temperature, 300 °C. Three replicates of each sample were performed in each polarity, and QC was randomly inserted in the batch to monitor the system stability over time. DI-FT-ICR analyses were performed in direct infusion nanoelectrospray mode using the automated multi-sample chip-based nESI sample ionization platform TriVersa NanoMate (Advion BioSciences Ltd, Ithaca NY, U.S.A), coupled to SolariX XR 7T (Bruker Daltonics, Bremen, Germany). The instrument was tuned with a standard solution of sodium trifluoroacetate NaTFA). Mass spectra were recorded in broad band mode in the range of 90–800 m/z, with an ion accumulation of 10 ms, and 32 scans were acquired using 2 million data points (2 M), with a resolution of 150.000 at m/z 400. The drying gas (N2) was set at 2 mL/min, with a drying temperature of 150 °C. The funnel amplitude was set to 90 V (polar metabolites) or 100 V (lipids), transfer was set at 0.6 MHz, and TOF 0.7 s. Both positive and negative ESI ionization were employed in separate runs. The instrument was controlled using a Bruker FTMS Control (Bruker). The detailed infusion conditions are reported in ESI.

4.11. *In vivo* polyphenol testing

SAMP and AKR mice were maintained under SPF conditions, fed with standard laboratory chow, and kept on 12-h light/dark cycles in the animal resource core (ARC) facility of Case Western Reserve University (CWRU). 5-week-old mice were divided into two groups: vehicle vs purple corn; the vehicle group received normal water while the purple corn group received 53 mg/kg [96,97] of the polyphenol powder dissolved in water, changed each day for 70 consecutive days. Mice were checked every day and weighed every week. At day 70 all mice were euthanized according to the ARC protocols and their small intestine and colon were explanted, fixed in Bouin's fixative (Sigma-Aldrich, St. Louis, MO, USA) for 24 h, and stored with 70% EtOH before paraffin embedding, sectioning and staining for histological analysis; staining was made with hematoxylin/eosin. Colon length and weight were measured as indicators of colonic inflammation at sacrifice. The colon/body weight indices were calculated as the ratio of the colon wet weight and the total body weight and as the ratio of the colon length and the total body weight of each mouse.

4.12. 16S rRNA microbiome analysis

Mouse stool was collected before (Day 0) and after the end of the purple corn treatment (Day 70). Following fecal DNA extraction using the QIAamp® PowerFecal® Pro DNA kit (QIAGEN, Hilden, Germany) according to the manufacturer's protocol; microbiome amplification for the 16s rRNA gene V4 regions and high-throughput 16S rRNA gene microbiome sequencing and analysis was conducted using the well-established Illumina MiSeq and analytical protocols as previously described [68].

4.13. Statistical analysis and metabolomics data processing

Statistical analysis was performed using the GraphPad Prism 8 software (GraphPad Software, San Diego, CA, USA). All data obtained from at least three independent experiments were expressed as mean ± SEM.

We evaluated statistical significance using the two-way ANOVA test following Sidak's post hoc test. The results were considered statistically significant at $p < 0.05$. The HRMS data analysis was performed with MS-DIAL v4.48 (http://prime.psc.riken.jp/compms/msdial/main.html) and MetaboScape 2021 (Bruker). The detailed processing parameters for both UHPLC-HRMS and FT-ICR peak picking, alignment, and annotation are reported in ESI. Metabolites were annotated based on the Metabolomic Standard Initiative19 criteria, where the largest part of the metabolites was annotated MSI level 2 with accurate mass/spectral similarity/isotopic fine structure, or where the standard was available on MSI level 1. For some cases where isomeric overlap occurred and/or in the absence of reference MS/MS spectra, the metabolites were annotated on level 3, and thus assigned to a biochemical class. Univariate and multivariate statistical analyses were conducted with normalized and scaled HRMS data using MetaboAnalyst (v. 5.0, http://www.metaboanalyst.ca/) and data from both ionization polarities were treated simultaneously. One-way ANOVA with the Tukey post hoc test was performed for intergroup comparisons with false discovery rate (FDR) correction. Two classification models were used to verify if the levels of the metabolites were different among the treatments, principal component analysis (PCA) and partial least square discriminant analysis (PLS-DA). PLS-DA was also used to graphically describe the class separation and to extract relevant metabolites defined as that showing variable importance in projection (VIP) score higher than 1.3. The validity and robustness of the PLS-DA model were evaluated using coefficient R2 (modelfit) and coefficient Q2 (predictive ability), respectively, using the 5-fold internal cross-validation method. Heat maps and whisker box plots were used to highlight the most significant metabolites. Enrichment and pathway analysis was performed with the relative tools in MetaboAnalyst 5.0.

Bioinformatics analyses of sequence data, from the processing of raw DNA sequence, reads to alpha index estimates were conducted in the QIIME2 microbiome

platform (version 2020.8). Paired demultiplexed 16S sequences have been denoised by using the q2-deblur QIIME plugin (https://github.com/qiime2/q2-deblur). Taxonomy has been inferred by using the SILVA QIIME-compatible classifier (release 138). Alpha diversity metrics including Shannon entropy and Faith's PD were also computed by using the QIIME2 platform [98,99]. Starting from QIIME2 relative abundances, the q2-emperor plugin was used to compute beta diversity metrics.

Significant taxa among groups were computed by using a two side Welch test corrected by multiple tests with Benjamini-Hochberg.

5. Results

5.01. Iron-enriched medium improves mDCs TNF secretion in response to LPS

During DCs maturation, iron uptake is important to support energy production, respiration, and metabolism. For this reason, we compared DCs' response to LPS in conventional or iron-enriched media. Briefly, bone marrow precursors of DCs were cultured in a conventional medium with mGM-CSF and mIL-4 for seven days. Immature mDCs were exposed to LPS for 24 hours before being harvested.

mDCs cultured with iron-enriched medium for the last 24 h (day 10 of culture) and activated with LPS consistently increased the secretion of the inflammatory cytokine TNF, while IL-1α, IL-1β, IL-6, and IL-12/23p40 were not affected (Figure 5 A). We did not observe any variation in cell viability too (Figure 5 B).

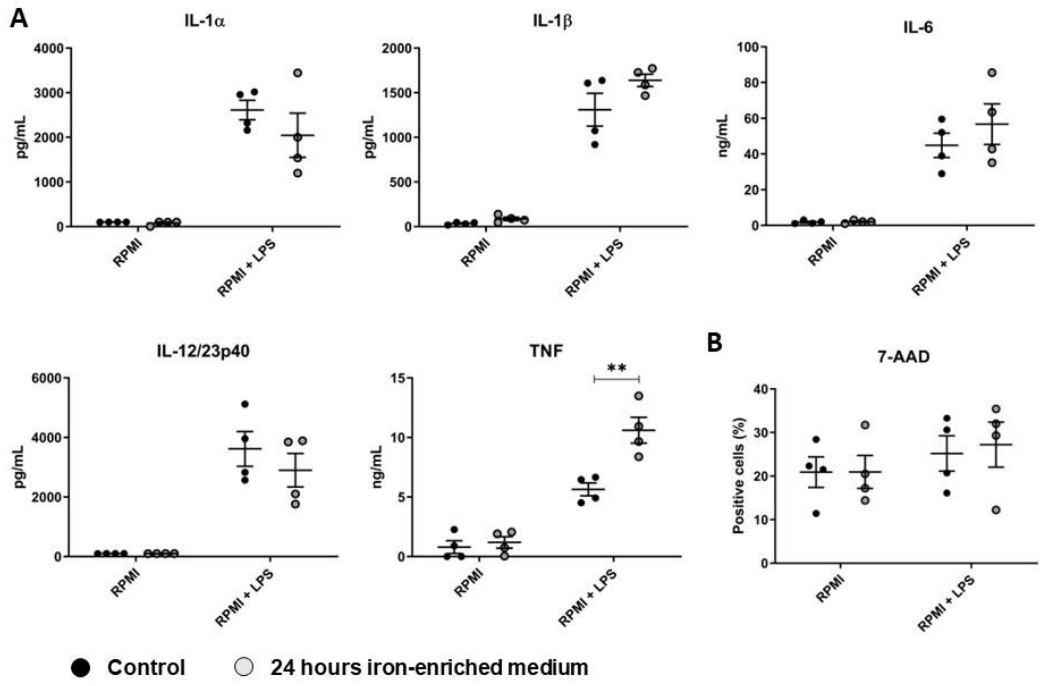

Figure 5. (A) Cytokine secretion by mDCs (n=4) cultured with iron for 24 hours. (B) Cell vitality analysis with 7-AAD staining. ** $p < 0.01$. Mean ± SEM is showed

These results indicate that iron is a necessary ion for mDCs. They need it to perform their activity and an increased concentration of this metal further boosts their effectiveness as observed with other immune cells [19].

5.02. Iron-enriched differentiating medium reduces inflammatory cytokine secretion by mDCs

Due to the crucial role of iron homeostasis in the inflammatory process, we evaluated whether culturing mDCs in an iron-enriched medium for seven days could improve the secretion of inflammatory cytokines. Briefly, mDCs were cultured in conventional or iron-enriched medium with GM-CSF and IL-4 for ten days. mDCs maturation was induced with LPS for 24 hours before harvesting them.

Surprisingly, cells grown for ten days in an iron-enriched medium significantly reduced inflammatory cytokines (TNF, IL-1β, and IL-6) secretion after LPS stimulation, while IL-1α and IL-12/23p40 secretions were not affected (Figure 6 A).

Cell vitality was not influenced by the excess of iron in the culture medium (Figure 6 B). These results could exclude the hypothesis that the observed reduction of inflammatory cytokine secretion was the result of a reduction in cell number.

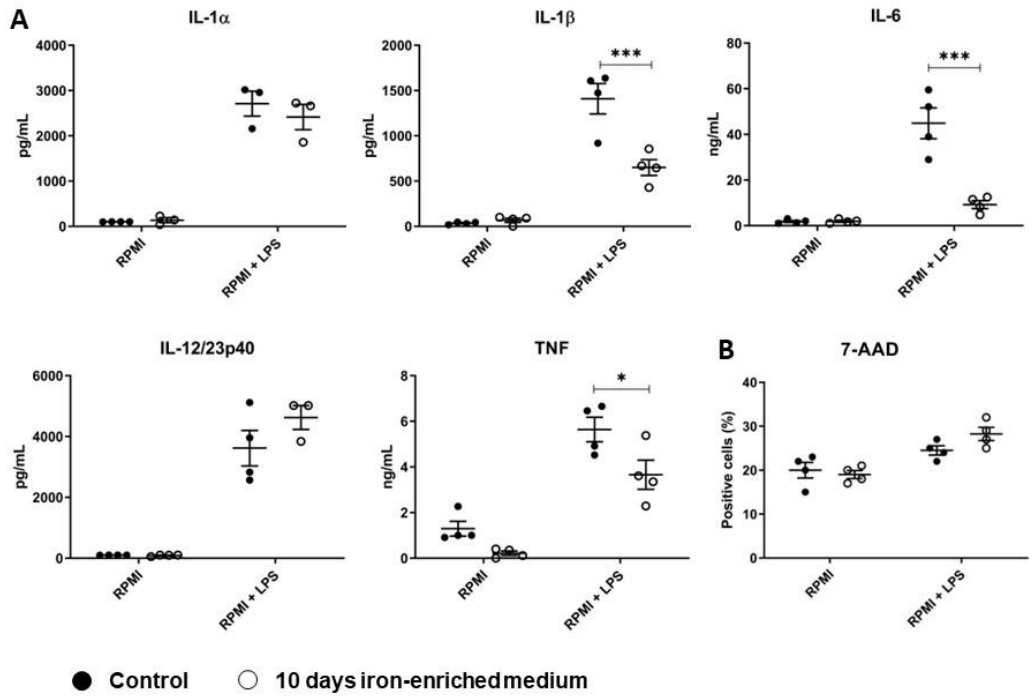

Figure 6. (A) Cytokine secretion by mDCs (n=4) cultured with iron for 10 days. (B) Cell vitality analysis with 7-AAD staining. * $p < 0.05$ *** $p < 0.001$. Mean ± SEM is showed

Differentiating bone marrow progenitors in an iron-enriched medium we mimicked iron overload conditions, what we obtained were functionally and phenotypically different cells to mDCs cultured in a conventional medium. Iron overload mimicking conditions did not affect cell viability but induced marked changes in cell phenotype and morphology. Cells appear to lose their differentiated potential and do not secrete proinflammatory cytokines like IL-1β, TNF, and IL-6. Nevertheless, IL-1α and IL-12/23p40 were still secreted by mDCs grown in an iron-enriched medium. This, combined with the 7-AAD low positivity in the samples, is a suggestion of the

presence of still vital cells that are not mDCs, possible monocytes, or undifferentiated DCs, but they are still able to respond to LPS [100,101].

5.03. mDCs cultured in an iron-enriched medium are smaller

At day ten, cells were treated with LPS and 24 h, and later they were imaged. When FITC-dextran was added to the culture medium (Figure 7 A, B), mDCs demonstrated endocytic abilities both in a conventional and iron-enriched medium as shown by the green fluorescence accumulated in the cytoplasm of mDCs matured with LPS. Hematoxylin staining highlighted the different morphology of the cells grown in iron-enriched conditions for ten days and stimulated with LPS compared to control cells stimulated with LPS (Figure 7 C–F). mDCs cultured in iron overload mimicking conditions appear significantly smaller (Figure 7 G).

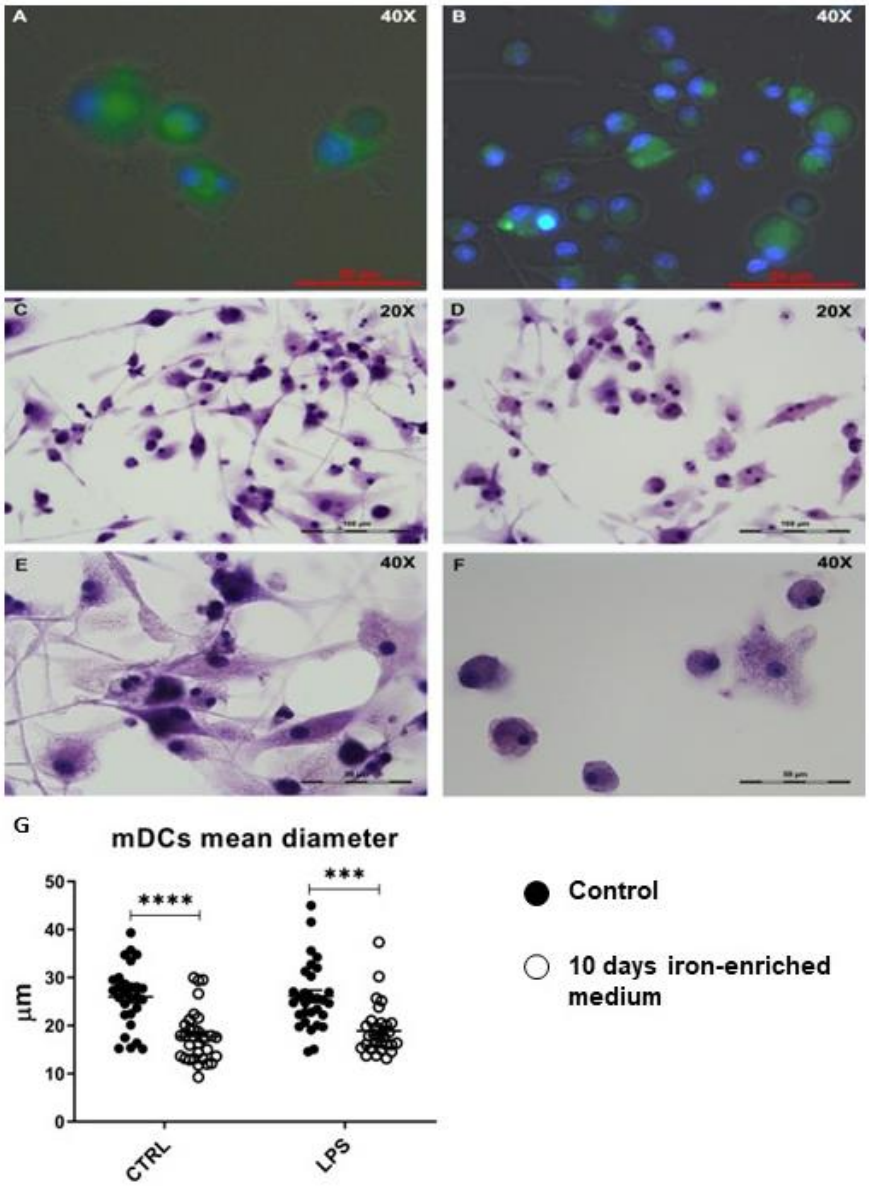

Figure 7. Representative images of FITC-dextran stained mDCs in control conditions (A), grown in iron-enriched medium (B). Brightfield images of control mDCs stained with hematoxylin (C, D) and mDCs grown in iron-enriched medium (E, F). mDCs dot plot with their mean ± SEM diameter (G). Images were taken with a 20× objective and a 40× immersion objective. *** $p < 0.001$ **** $p < 0.0001$

Microscopic imaging clearly shows live cells, confirming what we observed with the 7-AAD analysis. Cells grown in iron overload mimicking conditions, as well as their control counterparts, retain phagocytic ability characterizing mDCs and

monocyte/macrophages suggesting a role similar to iron-scavenger monocytes previously reported in the literature [102]. Morphologically, these cells appear smaller and possess fewer dendrites compared to control mDCs. The reduced cytoplasmic volume may partially explain the reduced secretory and antigen-presenting ability. This observed alternative phenotype may represent a defense mechanism against undesired chronic inflammation resulting from the excess of circulating labile iron.

5.04. Iron-enriched medium skews mDCs maturation towards $CD11c^+CD11b^+F4/80^+$ cells

We then characterized the surface phenotype of mDCs grown into an iron-enriched medium. It was immediately clear that there was a substantial enrichment in the $CD11b^+CD11c^+$ population in cells exposed to an iron-enriched medium for ten days (Figure 8 A). Gating on this population, we noticed that most of the $CD11b^+CD11c^+$ cells grown in an iron-enriched medium for ten days expressed F4/80 (Figure 8 B). Furthermore, cells cultured for ten days in an iron-enriched medium dramatically reduced MHCII expression (Figure 8 B).

We then exposed cells grown in both control and iron-enriched medium to LPS. LPS was unable to affect the $CD11c^+CD11b^+$ population percentage in cells grown in an iron-enriched medium for ten days (Figure 8 C). The percentage of $MHCII^+$ cells increased both in control and when the iron is given for 24 h (Figure 8 D). Cells cultured in an iron-enriched medium for ten days were not able to upregulate MHCII expression following LPS exposure like control cells (Figure 8 D).

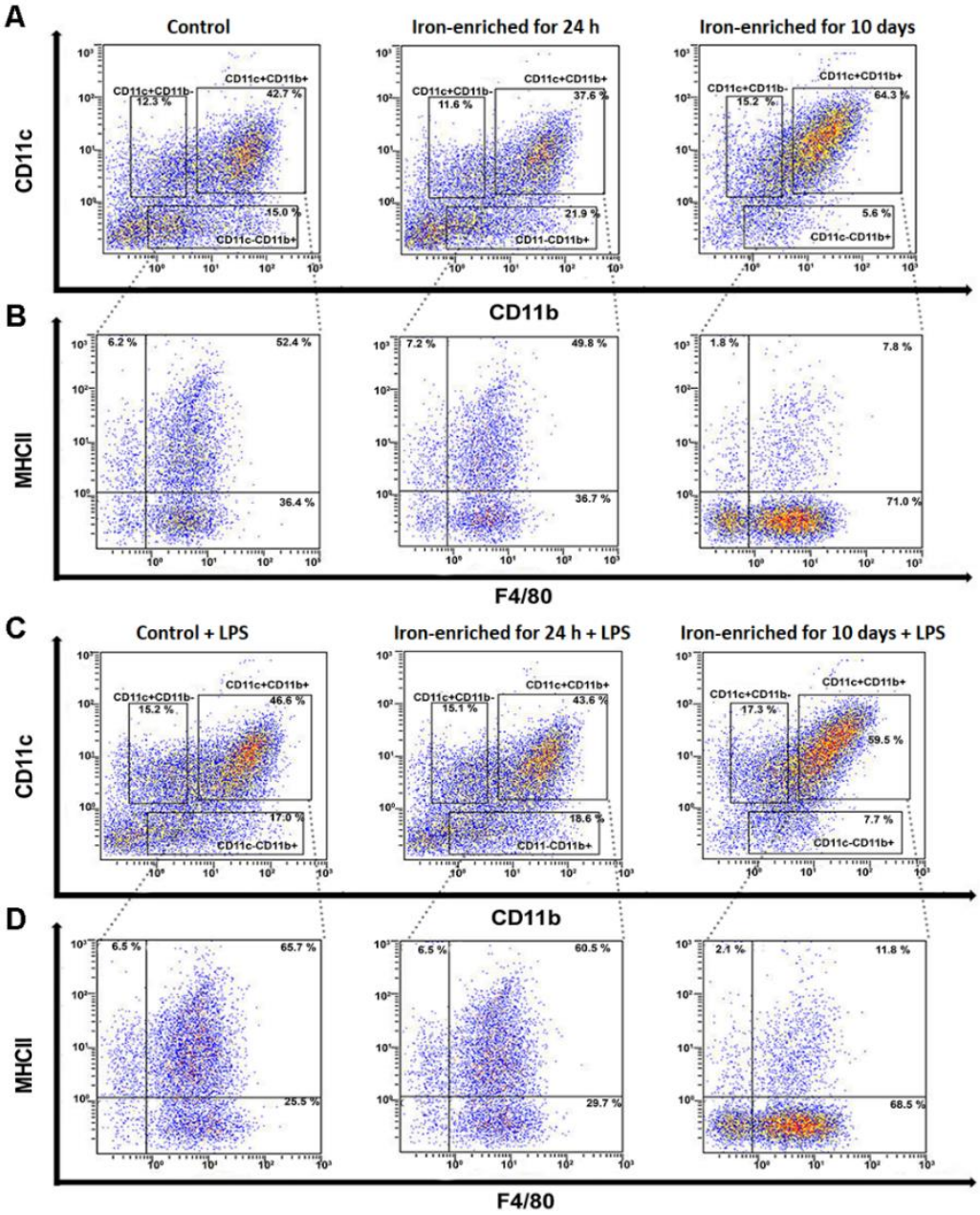

Figure 8. Representative density plots and histograms of mDCs cultured in an iron-enriched medium for ten days or 24 h (A, B). mDCs cultured in an iron-enriched medium for ten days or 24 h were exposed to LPS for 24 h (C, D).

FACS analysis revealed a significant reduction in canonical $CD11c^{+}MHCII^{hi}$ cells grown in an iron-enriched medium. Following ten days of culture in an iron-enriched medium, cells became $CD11c^{+}CD11b^{+}MHCII^{low}F4/80^{+}$ cells. Inorganic iron may

drive the expansion of macrophage-like cells resembling splenic red pulp macrophages [103]. Interestingly, this phenotype did not change when cells were stimulated with LPS compared to mDCs.

5.05. mDCs cultured in an iron-enriched medium for 10 days express *Tlr4* but poorly respond to LPS

We purified the mRNA from cells cultured as previously described to analyze the expression levels of crucial genes involved in mDCs development and response to LPS. mDCs cultured in a conventional medium resulted in $Irf8^{+}$, $Pu.1^{+}$, $Tlr4^{+++}$, and $Arg1^{+}$. Iron administration for 24 h did not significantly alter the expression levels of these genes. Despite the reduced response to LPS, the expression of *Tlr4* was not different between the three groups. On the other hand, *Irf8* and *Pu.1* expression was significantly lower than the one detected in cells cultured in a conventional medium, while the expression of *Arg1* was increased (Figure 9).

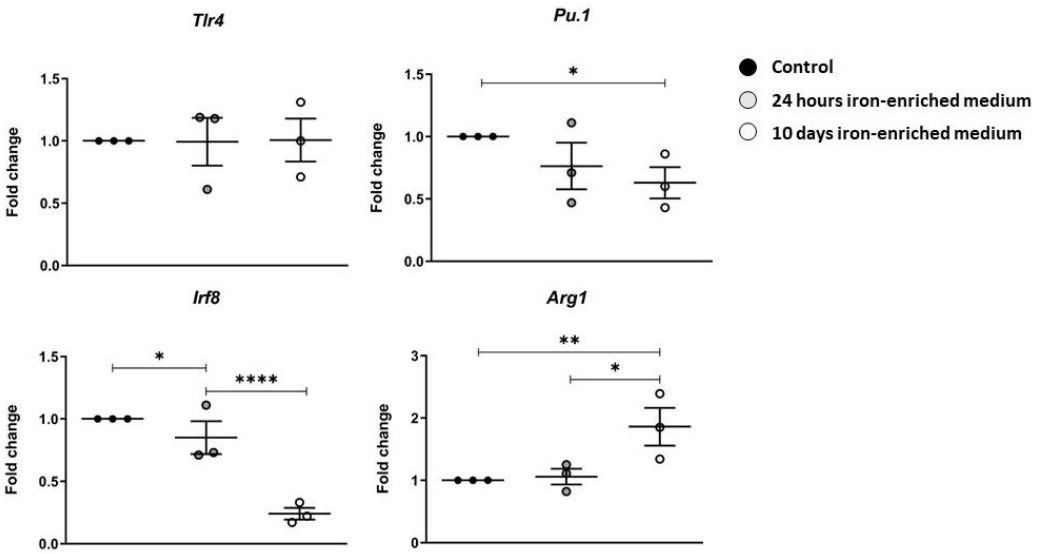

Figure 9. Gene expression analysis in control, iron-enriched medium for 24 h or 10 days, mean ± SEM is showed (n=3). mRNA was isolated 6 h post LPS exposure. * $p < 0.05$, ** $p < 0.01$, **** $p < 0.0001$.

In line with our speculation, at a molecular level, iron overload mimicking conditions favor the expression of *Arg1*, an enzyme mostly associated with monocyte and

macrophages that is downregulated during inflammation. Since mDCs differentiation is mainly driven by high levels of *Pu.1* and *Irf8* [104], we also studied these two genes, detecting a decrease in their expression in cells exposed to iron overload-mimicking conditions. This result suggests that bone marrow progenitors exposed to high iron concentrations fail to differentiate into mDCs and become alternative $CD11c^{+}CD11b^{+}MHCII^{low}F4/80^{+}$ cells, with a phenotype and a morphology similar to iron-recycling mono/macrophages. Thus, it becomes evident to provide the right amount of iron during therapies for anemia while maintaining it as low as possible to sustain a normal inflammatory response against pathogens; it is important to underline that iron is still necessary for our body and cells but its deprivation or its increased presence can lead to the opposite and detrimental effects. An important aspect that can be used to counteract an increased concentration of iron is the ability of polyphenols to chelate iron ions and deprive cells of this metal.

5.06. mDCs and pDCs response to LPS is modulated by quercetin

We generated pDCs and mDCs in vitro from murine bone marrow common precursors, with Flt3L and GM-CSF+IL-4, respectively.

Using cytofluorimetric analysis, we confirmed the efficient maturation of bone marrow progenitors into $CD11c^{+}B220^{+}Ly6C^{+}$ cells grown with Flt3L in the culture medium. Figures 10 A–E describe the different surface markers expression in cells cultured with GM-CSF+IL-4 ($CD11c^{+}B220^{-}Ly6C^{-}$ cells) versus Flt3L ones ($CD11c^{+}B220^{+}Ly6C^{+}$ cells). Of notice, cells cultured with Flt3L were approximately 20% $CD11c^{+}B220^{neg}$, 45% $CD11c^{+}B220^{int}$, and 25% $CD11c^{+}B220^{high}$ cells. Interestingly, 24 h after LPS stimulation, Flt3L cultured cells were 5% $CD11c^{+}B220^{neg}$, 35% $CD11c^{+}B220^{int}$, and 45% $CD11c^{+}B220^{high}$. These data indicate that even in the presence of heterogeneous cell culture, cells responded to LPS upregulating B220 surface expression.

pDCs can respond to LPS by upregulating the expression of MHCII, but not CD80 (Figure 10 F–G). In line with the aforementioned results, we detected *Tlr4* expression in pDCs (Figure 10 H) even if significantly lower than what was observed in mDCs.

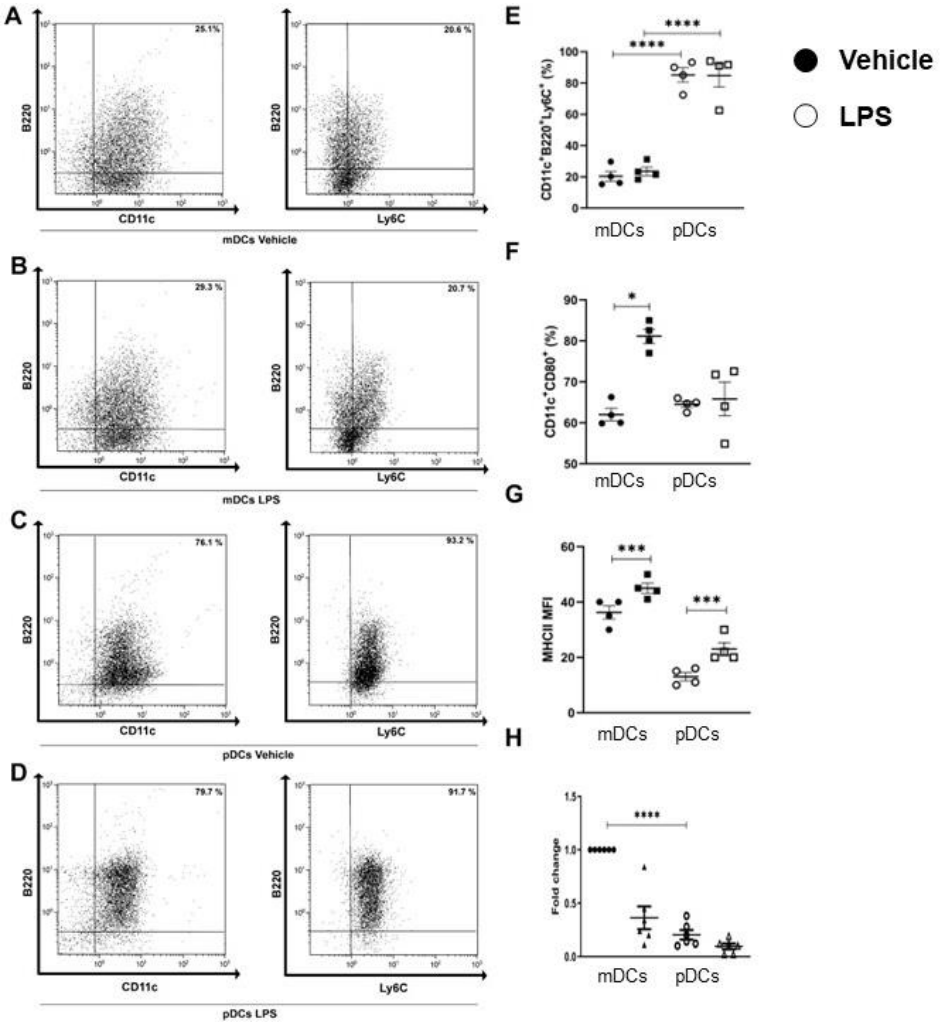

Figure 10. Representative density plots for CD11c, B220, and Ly6C staining in mDCs (A), myeloid dendritic cells (mDCs) stimulated with lipopolysaccharide (LPS) for 24 h (B), plasmacytoid dendritic cells (pDCs) (C), pDCs stimulated with LPS for 24 h (D). Bar plots for mean ± SEM (n=4) showing the percentages of $CD11c^{+}B220^{+}Ly6C^{+}$ cells (E), $CD11c^{+}CD80^{+}$ cells (F), and major histocompatibility complex II (MHCII) MFI (mean fluorescence intensity) (G) in control and after LPS stimulation for 24 h. Bar plots representing the mean ± SEM (n=6) of toll-like receptor 4 (*Tlr4*) gene expression relative to control mDCs (H). * $p < 0.05$ *** $p < 0.001$ **** $p < 0.0001$.

LPS was used as an inflammatory stimulus for pDCs. Response to LPS most commonly requires TLR4 expression [105,106]. The literature is not clear and often

discordant about the expression of TLR4 by pDCs; however, in our experimental setup, Flt3L cultured cells generate a heterogeneous population enriched in pDCs that can respond to LPS and secrete inflammatory cytokines. Flt3L cultured cells express lower but still detectable *Tlr4* mRNA. In these experimental conditions, we cannot exclude that the detected *Tlr4* is expressed by the 20% of $CD11c^{+}B220^{neg}$ cells observed; nonetheless, surface B220 upregulation and cytokine secretion strongly suggest that pDCs efficiently respond to LPS administration. Moreover, MHCII expression is significantly upmodulated when pDCs are exposed to LPS.

We tested the release of 22 cytokines by quercetin pre-exposed pDCs and mDCs 24 h after the activation with LPS. Vehicle-treated pDCs and mDCs were used as control. In line with what was previously described, quercetin administration was able to suppress the secretion of most of the inflammatory mediators shown in the panel. Of note, despite the reduced expression of *Tlr4*, pDCs responded to LPS stimulation by secreting higher amounts of IL-10, IL-12p70, IL-27, and TNF if compared to mDCs (Figure 11). Moreover, despite pDCs being the primary IFNα secretory cells, this cytokine was not detected in the pDCs culture medium after stimulation with LPS (Figure 11).

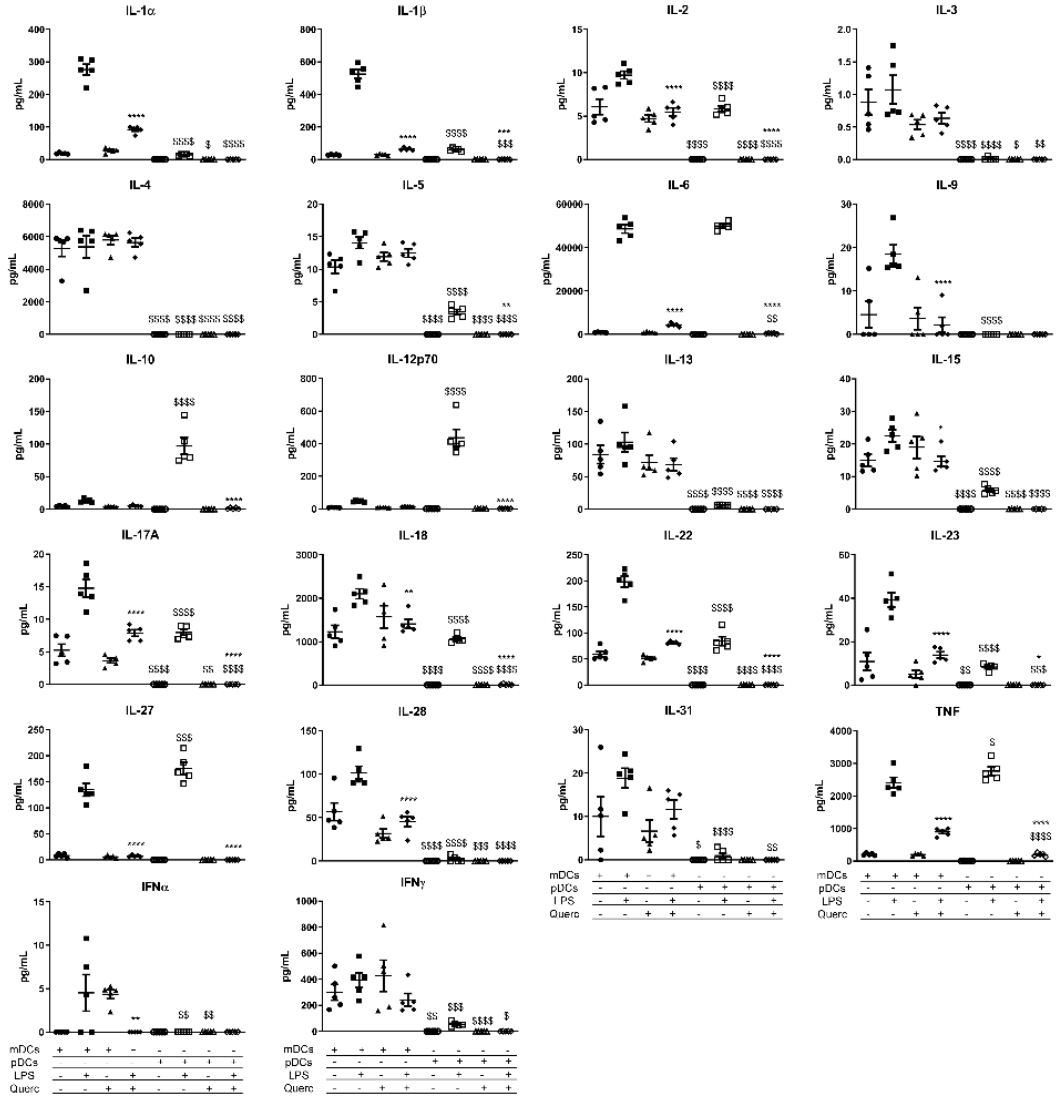

Figure 11. Scatter plots expressing the mean ± SEM (n=5) for secreted cytokines of mDCs and pDCs in baseline conditions and after stimulation with LPS and/or quercetin. *p<0.05 **p<0.005 ***p<0.001 ****p<0.0001; * LPS vs quercetin+LPS; $ mDCs vs pDCs

In line with our previous observations on mDCs, the panel of 22 cytokines provided useful insights on the inhibitory effects that quercetin has on inflammatory activity on DCs derived from different lineages. LPS activates the secretion of many cytokines in both cell types, with some cytokines differentially expressed and quercetin can suppress their expression in mDCs as well as in pDCs. Looking at

pDCs activated with LPS, our study shows surprisingly higher ability, even higher than mDCs, to secrete cytokines of the IL-12 family [107], in particular IL-12p70, IL-10, IL-27 following LPS administration. Quercetin pre-exposure completely suppressed cytokine secretion in pDCs with an efficiency that appears superior to what was observed in mDCs. Similarly, the secretion of IL-6, IL-18, and TNF is similar in LPS-stimulated pDCs and mDCs, but quercetin per-exposure is significantly more efficient in suppressing pDCs cytokine secretion than mDCs. Some of the selected cytokines, present in mDCs supernatants, are not secreted by pDCs; these include IL-3, IL-4, IL-9, IL-13, IL-28, IL-31, IFNα, and IFNβ. With these results we can assume that pDCs and mDCs perform non-redundant immunomodulatory activity after LPS stimulation, autoregulating their response to pathogens [108], but pDCs are more susceptible to quercetin pre-exposure.

To our surprise, pDCs stimulated with LPS did not secrete IFNα. That is indeed what was observed by Okada as LPS and TLR4 ligands did not activate IFNα secretion by DCs [109,110].

We also tested the secretion of growth factors, mDCs are the main producers of GM-CSF, G-CSF, M-CSF, and leukemia inhibitory factor (LIF); instead, pDCs secreted only a small amount of G-CSF, similar to mDCs after LPS administration (Figure 12).

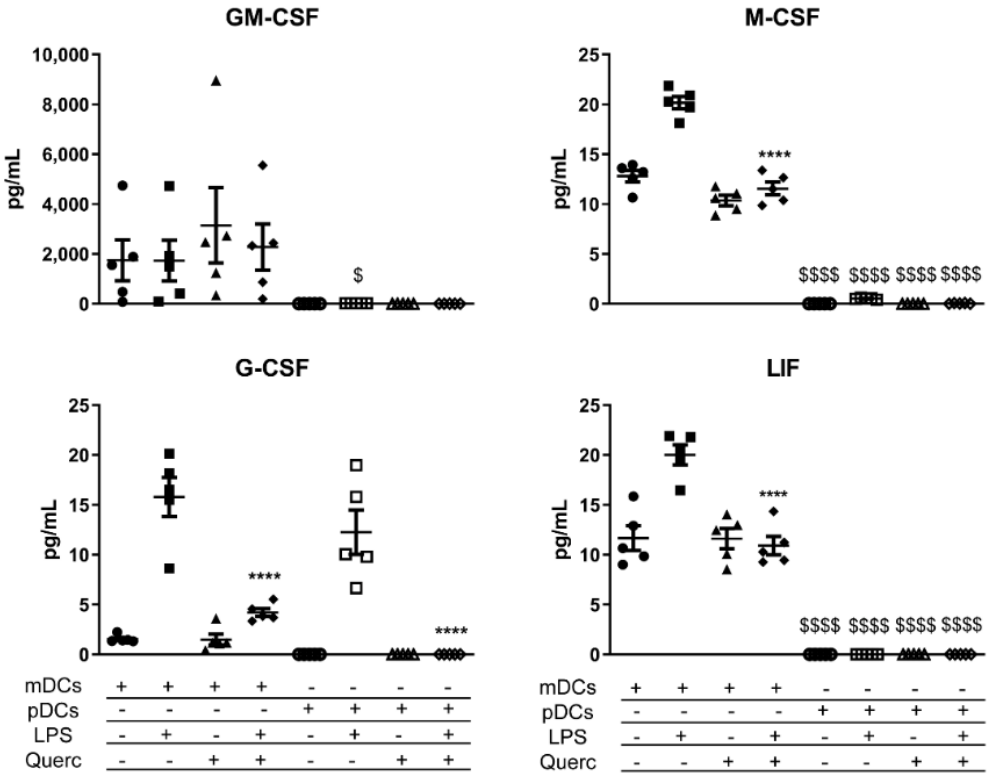

Figure 12. Scatter plots expressing the mean ± SEM (n=5) for secreted growth factors of mDCs and pDCs in baseline conditions and after stimulation with LPS and/or quercetin. * $p < 0.05$ **** $p < 0.0001$; $ $p < 0.05$ $$$$ $p < 0.0001$; * LPS vs. quercetin + LPS; $ mDCs vs. pDCs

Quercetin and polyphenols proved many times their anti-inflammatory and immunomodulating potential; however, little is known about their effects on pDCs. Here, we demonstrated that quercetin affects the inflammatory state of pDCs similarly to mDCs without substantially affecting cell vitality. Quercetin administration efficiently reduced the secretion of inflammatory cytokines from mature pDCs as well as mDCs.

In line with our previous observations on mDCs, the panel of 22 cytokines and growth factors provided useful insights on the inhibitory effects that quercetin has on inflammatory activity on DCs derived from different lineages. LPS activates the secretion of many cytokines in both cell types, with some cytokines differentially expressed, and quercetin can suppress their expression in mDCs as well as in pDCs.

Looking at pDCs activated with LPS, our study shows surprisingly higher ability, even higher than mDCs, to secrete cytokines of the IL-12 family [107], in particular IL-12p70, IL-10, and IL-27 following LPS administration. Quercetin pre-exposure completely suppressed cytokine secretion in pDCs with an efficiency that appears superior to what was observed in mDCs. Similarly, the secretion of IL6, IL-18, and TNF is similar in LPS-stimulated pDCs and mDCs, but quercetin pre-exposure is significantly more efficient in suppressing pDCs cytokine secretion than mDCs. Some of the selected cytokines present in mDCs supernatants are not secreted by pDCs; these include IL-3, IL-4, IL-9, IL-13, IL-28, IL-31, IFNα, and IFNβ. With these results, we can assume that pDCs and mDCs perform non-redundant immunomodulatory activity after LPS stimulation, autoregulating their response to pathogens [108], but pDCs are more susceptible to quercetin treatment.

The analysis of growth factors in both cell types displayed a marked difference in the secretion of G-CSF, M-CSF, GM-CSF, and LIF. To our knowledge, these factors induce the differentiation and the recruitment of neutrophils, macrophages, and other DCs; interestingly, there is evidence of a bias toward the differentiation of mDCs at the expense of pDCs when these factors are secreted at the site of inflammation [111-114]. Our data further demonstrate that mDCs recognize the threat of bacterial infection when stimulated with LPS and thus drive the immune response toward the recruitment of cells able to efficiently fight bacterial pathogens, while pDCs are more equipped to face viruses. In particular, the production of LIF is associated with the blocking of the differentiation toward pDCs [114].

5.07. Molecular characterization of mDCs and pDCs treated with quercetin

Using RT-qPCR, we analyzed the expression pathways in our experimental conditions. As expected, *Slpi* and *Hmox1* expressions were induced by quercetin in mDCs, while their expression was lowered in cells stimulated solely with LPS. On the same note, pDCs showed similar *Slpi* and *Hmox1* transcription modulation induced by quercetin and LPS (Figure 13).

We further examined the expression of interferon regulatory factor 7 (*Irf7*) and *Irf8* genes, which are both involved in the activation of downstream effector proteins of the inflammatory response and the regulation of the secretion of inflammatory cytokines. As expected, both genes were expressed in pDCs, to a lesser extent than in mDCs, and yet they are downmodulated by quercetin, even in the presence of LPS. Genes that regulate and modulate the inflammatory response and reduce oxidative stress, such as indoleamine 2,3-dioxygenase 2 (*Ido2*) and nuclear factor erythroid 2-related factor 2 (*Nrf2*), showed an increased expression in both mDCs and pDCs stimulated with LPS; however, *Ido2* levels are significantly lower in pDCs. Quercetin administration was able to reduce the cellular inflammatory state, as demonstrated by the significant reduction of the expression levels of both these genes. The molecular pathway induced by quercetin administration was independent of prostaglandin E receptor 2 (*Ptger2*) upregulation differently from what was previously reported in macrophages [115], but it involved a marked increase in the expression of activator protein 1 (*Ap-1*) mRNA, the transcription factor that regulates gene expression in response to LPS, in both cell types exposed to quercetin; only in mDCs, its expression gets significantly modulated when quercetin is used to counter the stimulation with LPS.

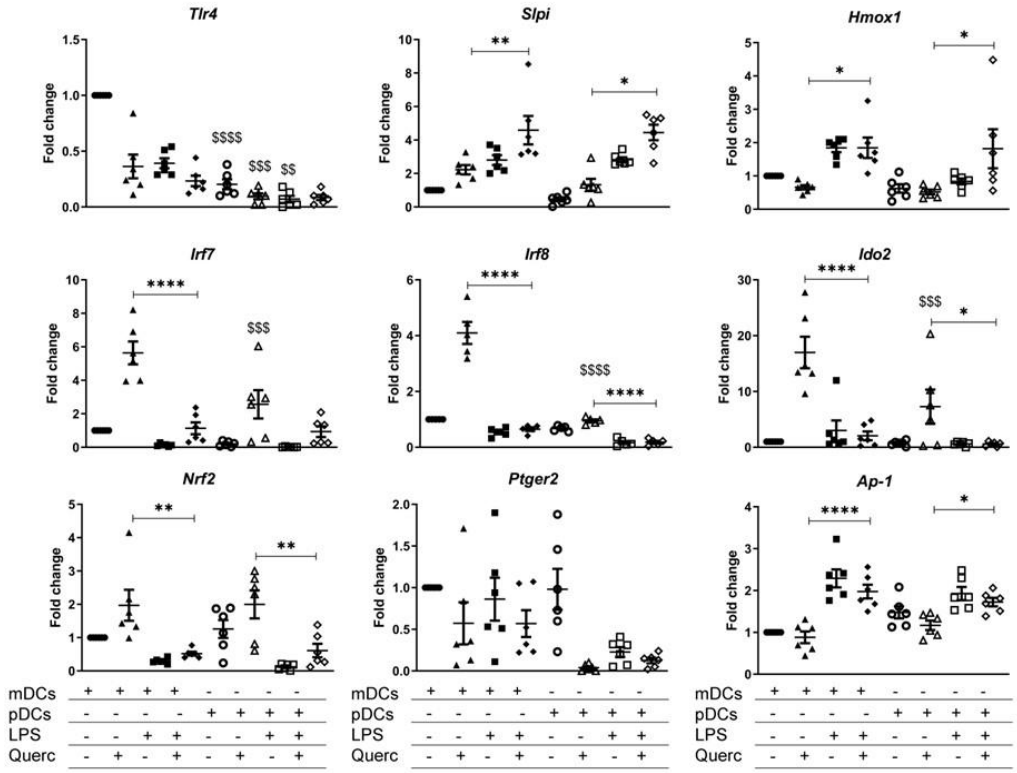

Figure 13. Molecular pathways activated in mDCs and pDCs 6 h after LPS stimulation and/or quercetin administration. Scatter plots expressing the mean ± SEM (n=6) of each gene expression relative to control mDCs. * $p < 0.05$ ** $p < 0.005$ **** $p < 0.0001$; $$ $p < 0.005$ $$$ $p < 0.001$ $$$$ $p < 0.0001$; * LPS vs. quercetin + LPS; $ mDCs vs. pDCs

We know that the *Slpi* gene is pivotal for controlling this molecular pathway, as Slpi-KO DCs fail to respond to quercetin exposure [25]. As we expected, *Slpi* expression was upmodulated by quercetin alone and when it was used to suppress the effects of LPS in both mDCs and pDCs. mDCs and pDCs express *Irf7* and *Irf8*, which are genes that regulate the expression of pro-inflammatory cytokines; LPS stimulation induced an upmodulation of both these genes. However, pDCs express significantly less *Irf8*, which is involved mainly in the production of type I IFN after viral infections. As confirmed by the cytokine expression of IFNα, we can deduce that LPS stimulation does not activate a sustained antiviral response in mDCs and pDCs.

Quercetin administration induced the expression of *Hmox1* and *Ap-1* [116], which are two genes involved in the reduction of oxidative stress and the secretion of inflammatory cytokines. Since quercetin increases *Slpi* activity and suppresses nuclear factor kappa-light-chain-enhancer of activated B cells (*NFkB*), we can propose and support our hypothesis, as *NFkB* and *Ap-1* act alternatively in the activation of downstream pro-inflammatory cytokine genes. Moreover, if *Ap-1* gets expressed when *NFkB* is suppressed, cells undergo a process of progressive inactivation and might initiate apoptosis processes [117]. Even though quercetin suppresses oxidative stress and cellular inflammatory response, *Nrf2* expression is lower in cells exposed to this polyphenol. Many studies support the thesis that *Nrf2* is overexpressed during oxidative stress and inflammation and gets upmodulated by quercetin, albeit this takes place in the initial stages after quercetin administration [118]. In the present study, we observed the downstream effect of its activation, with the reduction of the cellular inflammatory state and the expression of the *Nrf2*-related gene *Hmox1*. Lastly, *Ido2* modulation in both mDCs and pDCs is concordant with its role as a regulator of the inflammatory response; this gene indeed acts as a controller of cytokine secretion and "forbids" immune cells to secrete excessive amounts of cytokines, thus driving uncontrolled inflammatory responses [119,120].

5.08. *Humulus lupulus* anti-inflammatory effects on mDCs

We further tested the effects of *Humulus lupulus* fractions on mDCs activity. Their efficacy as anti-inflammatory compounds has been previously observed on NK cells [95], thus a need to explore more of their effect and characterize their potential on mDCs.

The fractioning resulted in three components that were composed of different secondary metabolites, in particular, fraction A contained hydroxycinnamic acids, flavonol-glycosides, and procyanidins, and fraction B was composed of α-acids, iso α-acids, and oxidized β-acids, with the main compounds being humulinone (20.14 ± 0.12 µg/mL), cohulupone (106.87 ± 0.3 µg/mL) and deoxycohumulone (38 .36 ± 0.26

µg/mL), while fraction C was rich in β-bitter acids such as adlupulone and lupulone (2.751 ± 0.03, 1.862 ± 0.07 µg/mL) and prenylflavonoids such as xanthohumol (65.49 ± 0.04 µg/mL). We administered different concentrations of HOP fractions (250, 125, 25, 12.5, and 6.25 µg/ml) to mDCs; following LPS stimulation for 24 hours, we observed a marked reduction in the secretion of IL-6 with HOP B and C fractions only when used at a concentration of 25 µg/ml (Figure 14 A). None of the fractions showed toxic effects at this concentration (Figure 14 B).

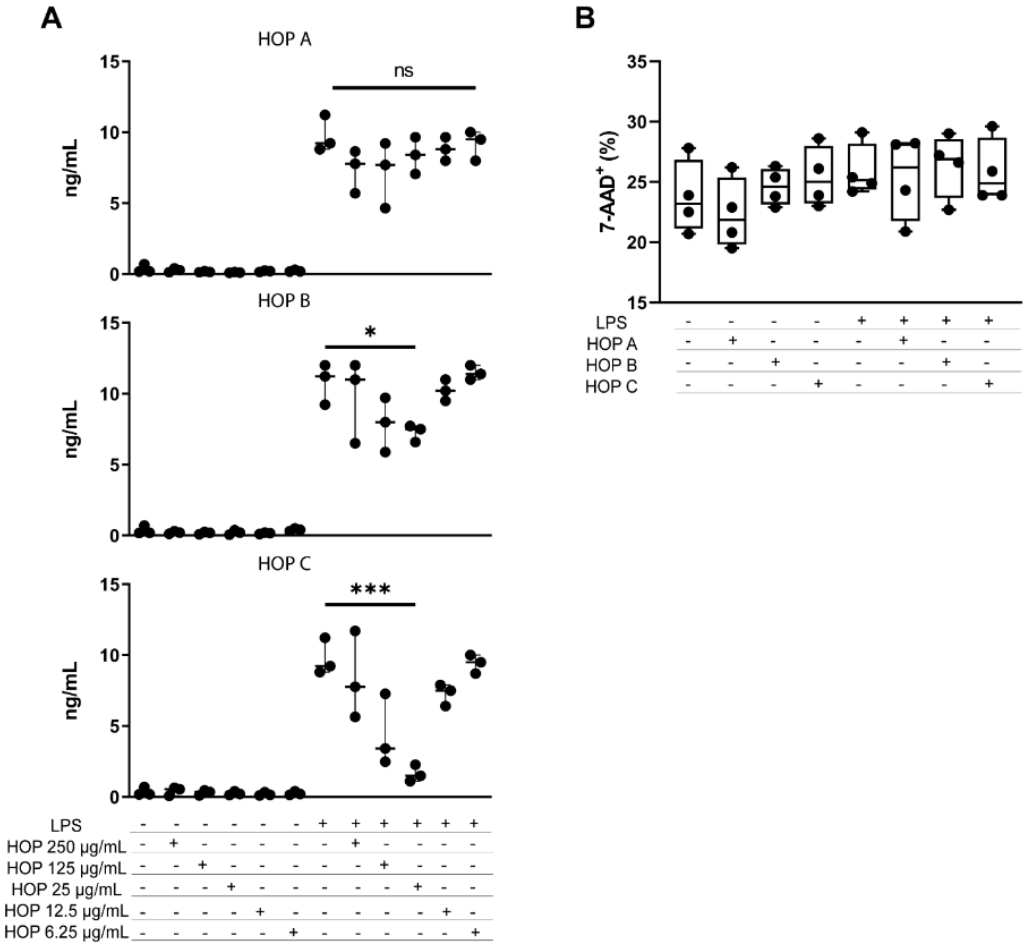

Figure 14. mDCs IL-6 secretion modulation by HOP A, B, and C fractions used at different concentrations (n=3). * p-value <0.05, *** p-value <0.001, ns non-significant (A). 7-AAD staining showing the percentage of dead cells in control conditions and after the administration of LPS and/or HOP A, B, or C fractions (B) (n=4). Scatter plots expressing the mean ± SEM

mDCs stimulated with LPS pre-exposed to 25 µg/ml of HOP B and C fractions showed reduced production of several inflammatory cytokines including IL-6, IL-1α, IL-1β, and TNF. The HOP C fraction was significantly more effective than the B fraction and therefore selected for further evaluation (Figure 15). The observed difference in the efficacy of the two Hop fractions suggests that their components have different anti-inflammatory potentials on DCs. β-Acids and prenylflavonoids such as xanthohumol show strong antioxidant and immunomodulatory potential against infection and metabolic syndromes [121,122].

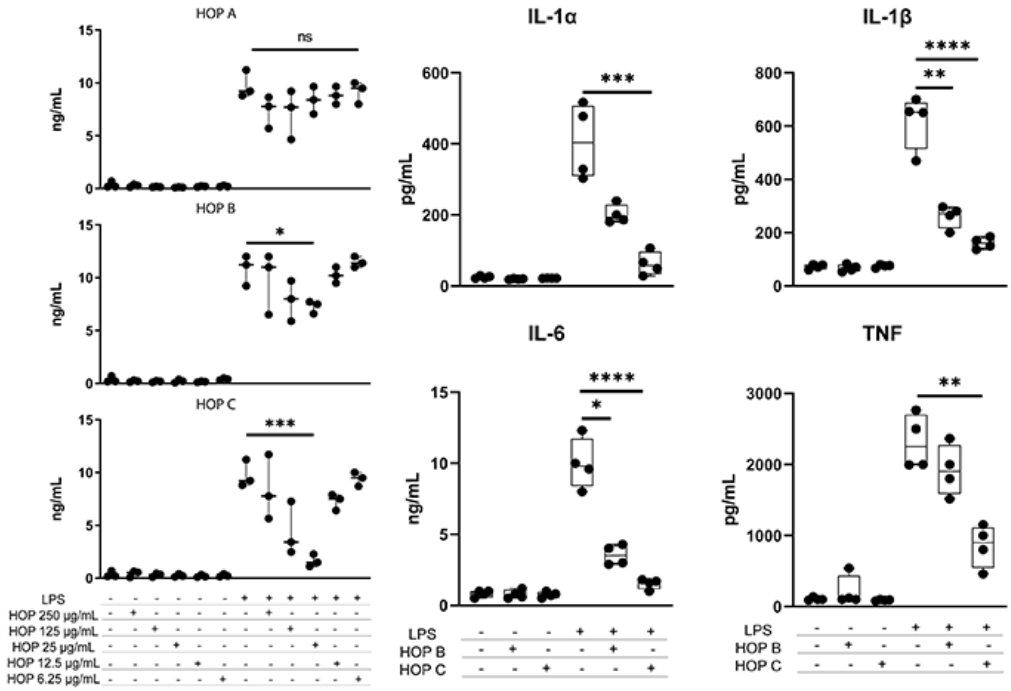

Figure 15. mDCs cytokine secretion modulation by HOP A, B and C fractions. * p<0.05, **p<0.005, ***p<0.0005, ****p<0.0001. Scatter plots expressing the mean ± SEM (n=4)

Recent evidence demonstrated that quercetin's ability to suppress mDCs inflammatory response to LPS was dependent on its ability to sequestrate extracellular iron and, consequently, reduce cytoplasmic iron concentration [43]. We administered the same concentration of HOP fraction C to mDCs with or without 2 µM iron in the culture well. Compared to quercetin, used as experimental control,

iron did not interfere with HOP C anti-inflammatory effects (Figure 16); whereas quercetin administration was not able to suppress inflammatory cytokine secretion when administered in an iron-enriched culture medium.

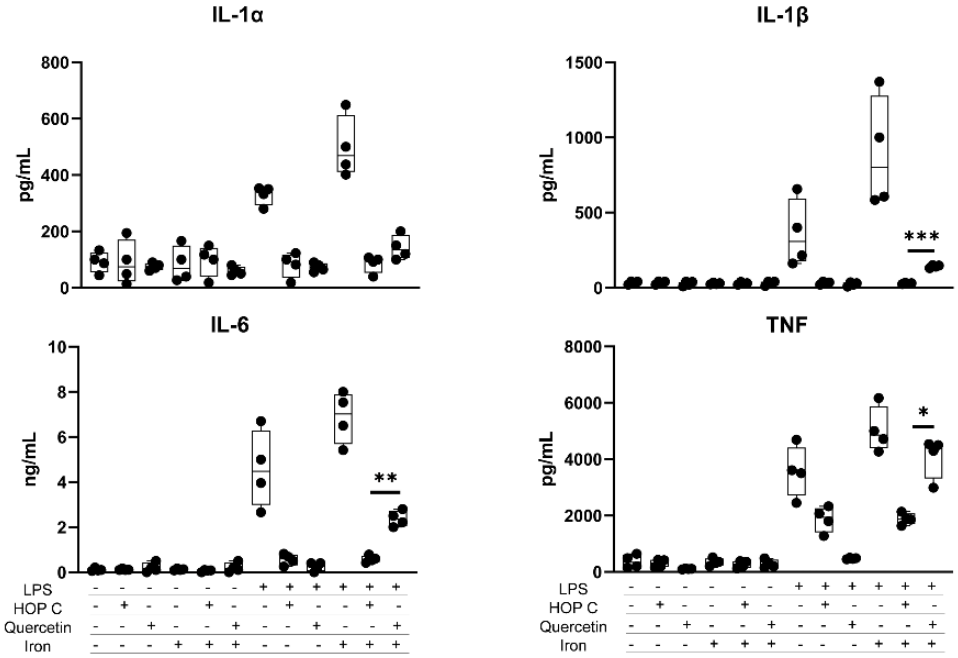

Figure 16. mDCs cytokine secretion modulation by quercetin and HOP C fraction with or without iron supplementation in the culture medium. * $p<0.05$, ** $p<0.005$, *** $p<0.0005$. Scatter plots expressing the mean ± SEM (n=4)

5.09. Molecular pathways modulated by quercetin and Hop C fraction

Although the inflammatory cytokine secretion suppression was similar in the HOP C and quercetin-exposed mDCs, the observation that HOP C inflammatory suppression was not related to iron sequestration suggests that the pathway activated by these compounds may be different. We tested the expression of several pivotal genes that regulate the anti-inflammatory abilities of quercetin in the HOP C-exposed mDCs (Figure 17). As expected, quercetin, not HOP C exposure, upregulated *Ferroportin* and *Hmox1* gene expression. Interestingly, the HOP C pathway is *Slpi*-independent, further highlighting the differences between HOP C and quercetin. HOP C showed significant upregulation of the *Nrf2*/*Nqo1* pathway and *Ap-1* compared to the unstimulated and quercetin-exposed mDCs, indicating an

anti-inflammatory and antioxidant pathway different from that induced by quercetin. The *Nrf2* pathway activates a quick antioxidant mechanism following LPS stimulation and

modulates important metabolic pathways that regulate glucose metabolism and produce substrate for the TCA cycle (tricarboxylic acid cycle) and mitochondrial respiration [123]. This is compatible with a return to a resting state in immune cells given that they reinstate the TCA cycle and aerobic ATP synthesis [124,125].

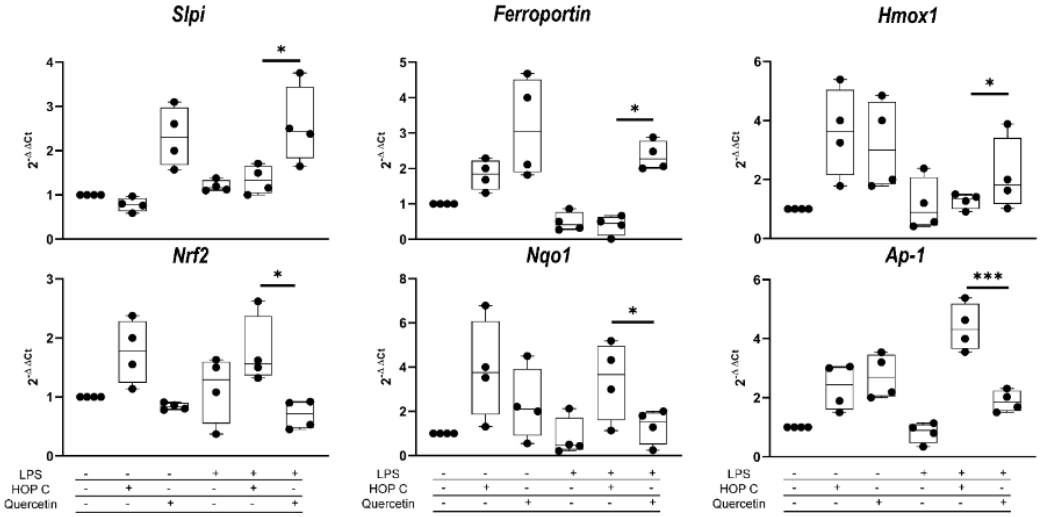

Figure 17. DC gene relative expression modulation by quercetin and HOP C fraction. * $p < 0.05$ and ***$p < 0.0005$. Scatter plots expressing the mean ± SEM (n=4)

Our results discriminate between two major anti-inflammatory and antioxidant molecular pathways, both influenced by quercetin and HOP C. We previously demonstrated that quercetin suppresses the inflammatory activity of mDCs by upregulating *Slpi* and its downstream *NF-κB* inactivation while reducing the intracellular iron content through the increased gene expression of *Ferroportin*. Alternatively, HOP C does not significantly induce the gene expression of *Slpi* and it does not influence the iron metabolism in mDCs. Its beneficial effects involve the activation of *Nrf2* and its downstream antioxidant genes such as *Nqo1*. Moreover, *Nrf2* regulates cellular energy production and aerobic glycolysis in the mitochondria, while protecting cells from ROS byproducts [126]. Nrf2 activation also increases

nicotinamide adenine dinucleotide phosphate (NADPH) and nicotinamide adenine dinucleotide (NADH) regeneration through the activation of *Nqo1*, further boosting oxidative phosphorylation (OXPHOS) energy biosynthesis and providing more intermediates to the mitochondria [127]. *Nqo1* is also responsible for the degradation of Iκb and the consequent suppression of inflammatory cytokine secretion [128]. The *Nrf2* downstream molecular pathway can direct cellular metabolism to a more conservative and stable condition, compatible with a resting state in cells and with an anti-inflammatory switch in immune cells. Furthermore, *Ap-1* is up-modulated by quercetin and its effects are pushed forward by Hop extracts, suggesting that this polyphenolic mixture can activate the *Nrf2*/*Ap-1* circuitry in mDCs and protect them from oxidative stress [129].

5.10. Untargeted metabolomics of mDCs treated with quercetin or HOP C

To gain further insight into the metabolic modulation of HOP C exposed mDCs, we performed an untargeted metabolomic analysis, resulting in 179 annotated metabolites, which were mainly divided into amino acids, peptides, and analog (21%); carbohydrates and carbohydrate conjugates (4%); carboxylic and dicarboxylic acids and derivative (2%); fatty acyls [FA] (17%); glycero- [GL] and glycerophospholipids [GP] (30%); organic acids, organonitrogen and organooxygen compounds (4%); pterins, purine and pyrimidines derivatives (11%); sphingolipids [SP] and sterols [ST] (7%) and others (4%).

Based on the results of inflammatory cytokines we divided the mDCs samples into four groups: control (CTRL), LPS-stimulated DCs (LPS), LPS-DCs plus HOP C (LPS+H), or quercetin (LPS+Q). LPS stimulation changed the mDCs metabolome as well as the treatment with HOP C or quercetin further modulated the metabolism of mDCs cells (Figure 18).

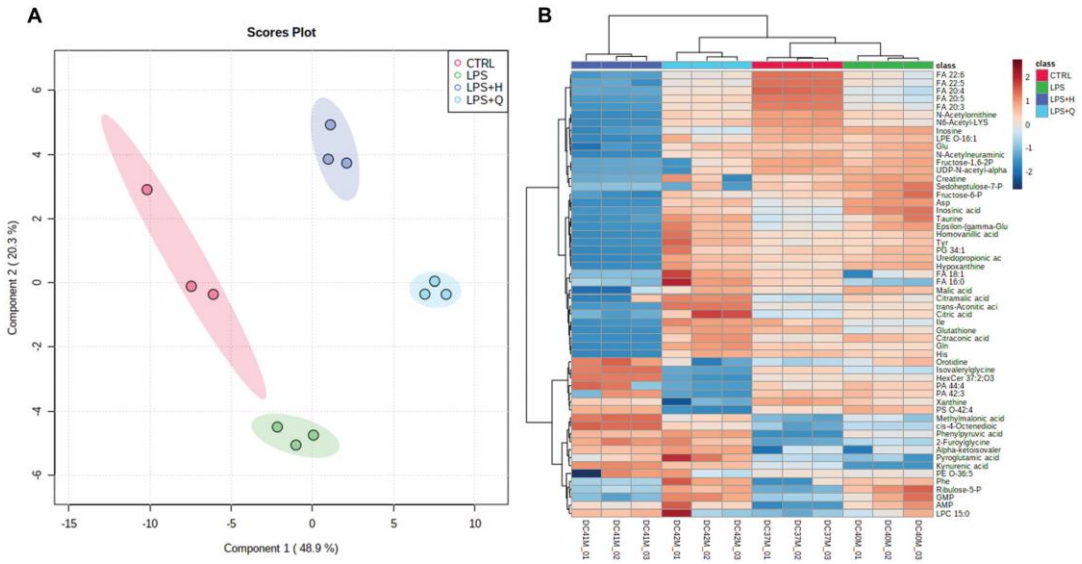

Figure 18. PLS-DA score plot (A) and heat map (B) of statistically relevant (ANOVA, $p < 0.05$) DC metabolites modulated by LPS, HOP C, and quercetin. (n=3)

In analogy to macrophages, the stimulation of mDCs with LPS induces a metabolic change towards an inflammatory phenotype [130] which is characterized by a shift from oxidative phosphorylation to aerobic glycolysis, with results in a decrease in TCA while lactate production and pentose phosphate pathway (PPP) increase, that leads to an increased biosynthesis in purine and pyrimidines to fulfill the energy demand [131]. In our model, numerous hallmarks of this metabolic shift were evidenced after stimulation with LPS (Figure 19). PPP is a key pathway for the production of NADPH for the NADPH oxidase enzyme, which produces ROS, and it is divided into oxidative and non-oxidative steps [132]. LPS stimulation both intermediates such as sedoheptulose-7-phosphate (S7P), and ribulose-5-phosphate (Ru5P) as well as end products fructose-6-phosphate (F6P) were increased. Interestingly, the level of these products was decreased with both HOP C and quercetin treatment, but the reduction of intermediates S7P and Ru5P and of the end product F6P were more pronounced after treatment with HOP C, suggesting that HOP C could modulate both non-oxidative and oxidative steps of PPP (Figure 19) compared to quercetin, which is known to increase glucose 6-phosphate levels [133].

On the other hand, quercetin does not affect F6P and R5P levels, suggesting a blockade of PPP as it is no more needed to provide energy to activated DCs or reducing molecules like NADPH [134].

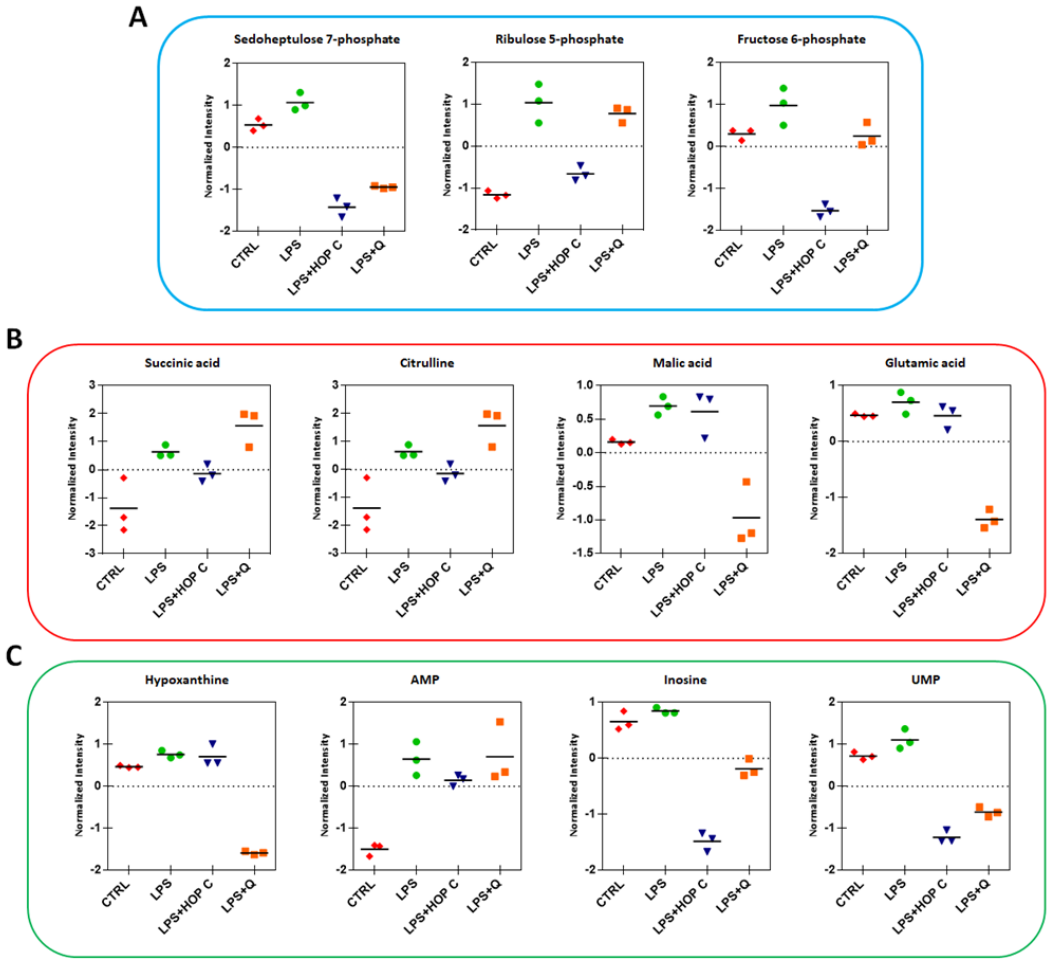

Figure 19. Normalized intensity of relevant metabolites altered involved in metabolic reprogramming of LPS-DCs and modulated by HOP C and quercetin treatments: (A) PPP intermediates, (B) TCA cycle, and citrulline, (C) Purine/Pyrimidines and Nucleotides. (n=3)

As also reported previously, the dysregulation of the TCA cycle induces the accumulation of some metabolites, in particular succinate, which has been recently identified as a key signaling metabolite during inflammation by activation of the hypoxia-inducible factor-1α (Hif-1α) transcription factor and subsequent enhancement of IL-1β production [135]. LPS-stimulated mDCs showed an increased

level of succinate. mDCs treated with HOP C or quercetin both displayed a significant reduction of succinate levels compared to LPS status, but this effect was more marked with Fraction C when compared to quercetin (Figure 19), furthermore, glutamate and malate (Figure 19) reduction was more pronounced in cells that received quercetin. On the contrary, mDCs treated with HOP C displayed a significant reduction of succinate levels, greater when compared to quercetin, while glutamate and malate reduction was more pronounced in quercetin-treated mDCs (Figure 19). TCA intermediate reduction in quercetin-treated mDCs might be a consequence of iron deprivation as it was observed in macrophages [136]. Strikingly, opposite effects were observed, with HOP C-treated mDCs that reduced L-citrulline levels, while in quercetin-treated mDCs L-citrulline level was higher than LPS alone, indicating an opposite response (Figure 19). These aspects could point out a potential peculiar effect of HOP C in reducing inflammation by regulation of arginine-citrulline and arginine-succinate cycles that are increased during inflammatory status to sustain TCA cycle anaplerosis [137]. The increase in PPP boosts also the production of purine and pyrimidines, for biosynthetic and energy processes in the cell [124]. As a result, in LPS, treated mDCs a profound dysregulation of purine and pyrimidines metabolism was observed, in particular hypoxanthine, inosine, cytidine, and adenosine were all increased (Figure 19), as well as several nucleotides. A different modulation trend was observed in mDCs treated with HOP C and quercetin, in particular, hypoxanthine and inosine monophosphate (IMP) levels were more reduced in quercetin-treated mDCs, while AMP and inosine and uridine monophosphate (UMP) were higher when compared to HOP C exposed mDCs (Figure 19). Noteworthy, the increased AMP in LPS-treated mDCs, suggests an accelerated breakdown of ATP, and an indication of increased energy metabolism through glycolysis, which was partially normalized with HOP C treatment. Our results suggest that hop bitter acids effectively impairs the inflammatory response by regulating the metabolic reprogramming of mDCs toward anti-inflammatory

conditions using different intracellular pathways compared to quercetin, which may be further exploited to suppress excessive inflammatory responses.

5.11. *In vivo* effects of polyphenol administration in a model of CD

Polyphenols have proved many times beneficial in reducing chronic colitis and we recently tested purple corn anthocyanins on human CD patients [138]. With that in mind, we tried the same powder on SAMP mice to see if that can influence their phenotype.

Young SAMP and AKR (used as control) mice were divided into two groups each starting at 5 weeks of age. The purple corn groups received 53 mg/kg of mouse weight of purple corn powder dissolved in sterile water, while the vehicle groups got plain water. The anthocyanin administration lasted for 70 days, and the solution was changed each day.

Mice were weighed every week and their growth curve can be seen in Figure 20 A-B relatively for SAMP mice and AKR mice.

At sacrifice mouse colon and small intestine were harvested, colon length and weight were measured and then they were processed for histologic analysis. Figure 20 C-D shows the colon weight to body weight ratio and the colon length to body weight ratio.

Histology scores from both ileum (Figure 20 E) and colon (Figure 20 F) show differences between the groups only for the ileum, according to the model used. Figure 20 G shows the reduced number of tertiary lymphoid organs (TLO) in SAMP mice treated with purple corn.

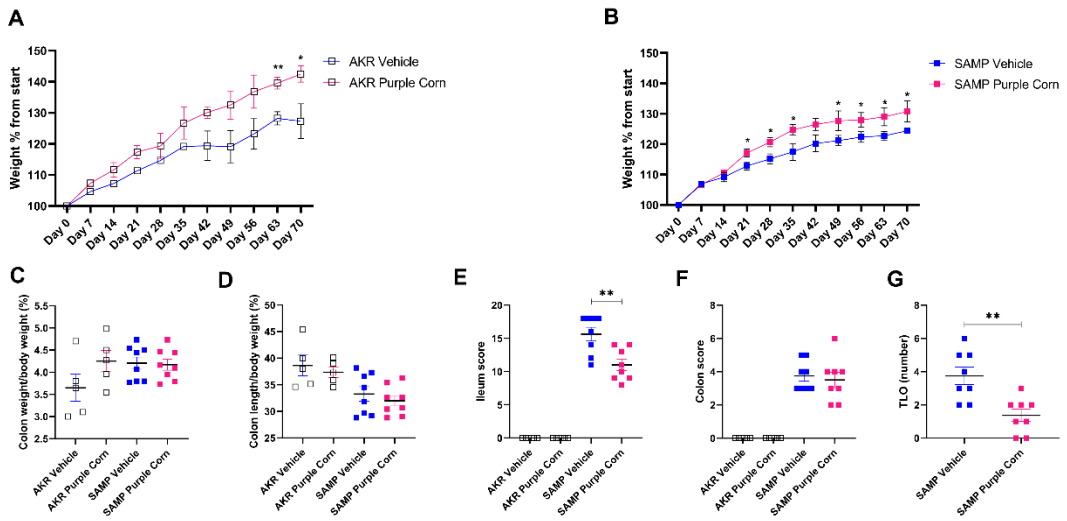

Figure 20. Experimental and sacrifice data of purple corn administration to SAMP (n=8) and AKR (n=5) mice for 70 days. (*p-value<0.05, **p-value<0.005). Mean ± SEM is showed

Histology analysis of the ilea of the purple corn-treated SAMP mice clearly shows a reduction of the inflammatory milieu with less immune cell infiltrate and a more conserved villi architecture. Vehicle-treated SAMP mice show more necrotic areas and larger immune cell infiltrates. AKR mice did not show any difference between the two groups (Figure 21). Purple corn administration to SAMP mice resulted in a marked decrease in SAMP disease. Ileum histologic score significantly decreased as can also be seen with the microscopic pictures as less immune cell infiltrate is present there and the villi appear less distorted than vehicle-treated SAMP mice.

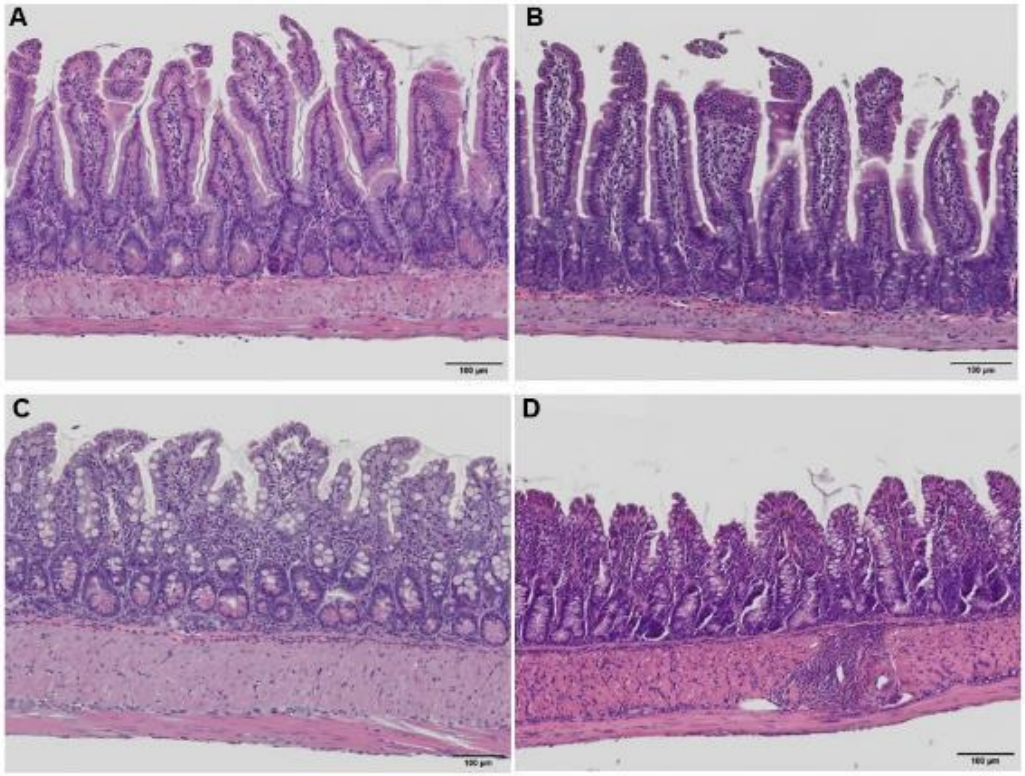

Figure 21. Microscopic images of representative ileum of vehicle-treated AKR mice (A), purple corn-treated AKR mice (B), vehicle-treated SAMP mice (C), and purple corn-treated SAMP mice (D), 10X magnification

Looking at TLOs, vehicle-treated SAMP mice present an increased number of them, mainly in the distal part of the colon while purple corn could reduce their number in all the SAMP.

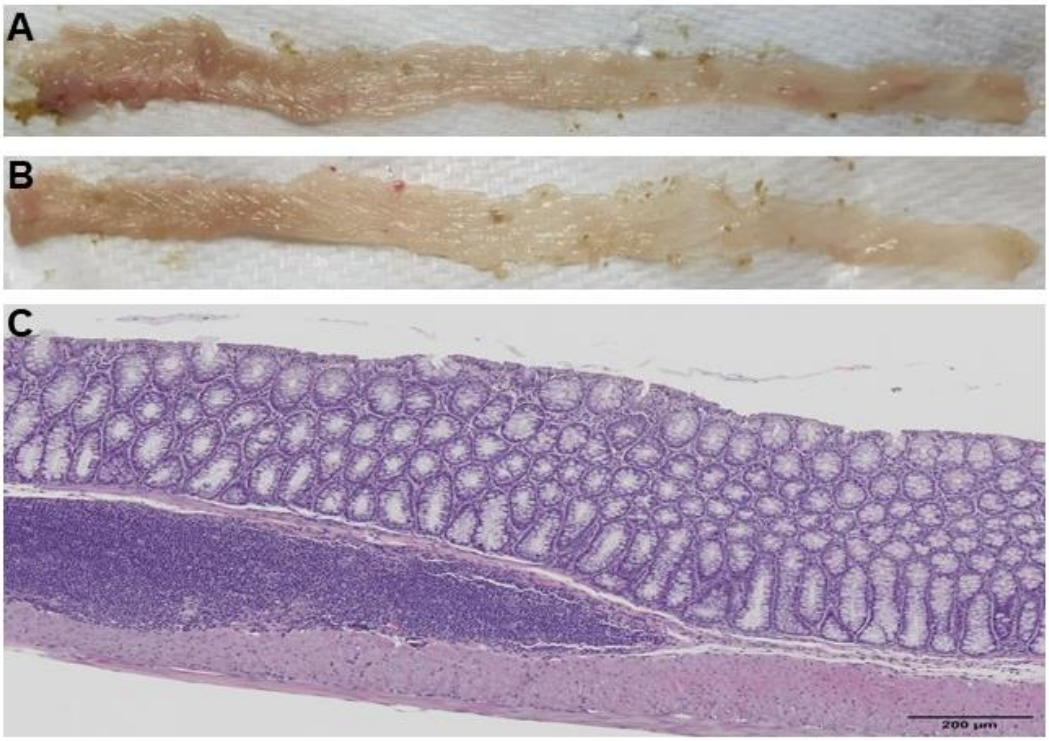

Figure 22. Representative pictures of a vehicle-treated SAMP colon (A) and a purple corn-treated SAMP colon (B). Microscopic image of a TLO (C), 10X magnification

Moreover, purple corn administration reduced the number of TLOs present in the SAMP colon, indicating that inflammation is also reduced in their colon even though we did not see any differences in the histologic score. TLOs however, are associated with IBD but whether they play a protective role or not is still debated [139].

Then, we performed a metagenomic analysis on 16S rRNA from stool taken from each mouse before the anthocyanin treatment (Day 0) and before the sacrifice (Day 70).

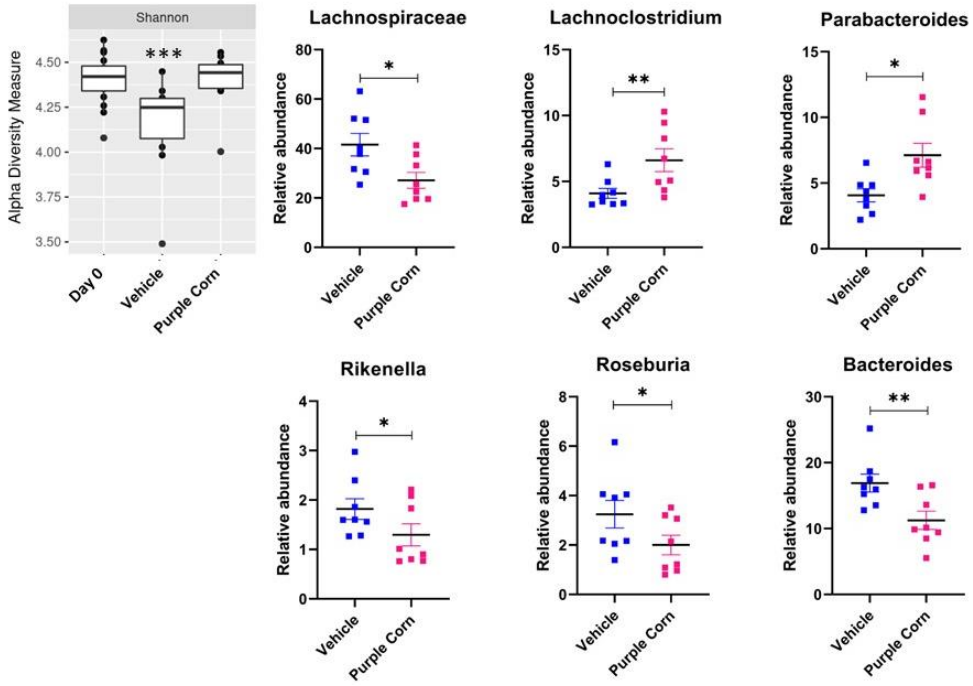

Figure 23. Shannon index box plot relative to SAMP mice (A), dot plots for the significant family (B), and genera (C-G) found in SAMP stool after 70 days of purple corn treatment. (*p-value<0.05, **p-value<0.005, ***p-value<0.001). Mean ± SEM is showed

After 70 days of purple corn treatment, the SAMP mice microbiota changed (Figure 23). There is less diversity according to Shannon's index and we observed changes in the Lachnospiraceae family and some genera. Lachnospiraceae are often responsible for IBD pathogenesis and are increased in CD patients and they can be influenced by polyphenols [140,141]. Parabacteroides were also found to be upmodulated after the administration of polyphenols, and their role in the gut is often regarded as protective and anti-inflammatory [142,143]. The Lachnoclostridum genus was found more abundantly in blueberry-treated rats, an indication that anthocyanin-rich foods might increase their presence and role in intestinal homeostasis [144]. Rikenella and Roseburia genera are related to IBD and inflammation and there is

evidence of anthocyanin modulation of their presence [145-147]. Lastly, the Bacteroides genus was found to have a predominant role in SAMP ileitis pathogenesis [148] and is often associated with an inflamed gut. AKR mice did not show any significant changes in their microbiota composition.

Purple corn proved useful in reducing inflammation in the SAMP model of CD. However, it cannot function alone, and it might be useful as an adjuvant to treatment with biological agents.

6. Conclusions

A right balance between iron intake and polyphenols is needed to prevent intestinal inflammation and, at the same time, the right tolerance towards non-pathogenic antigens. High or low amounts of iron have detrimental effects on health and the functioning of immune cells, thus the need to balance its intake, considering that many other foods might reduce iron absorption. Nevertheless, it is possible to modulate immune cell functions using polyphenols to reduce their inflammatory activity.

Metabolic and molecular pathways provided good insights into what can be exploited in the treatment of chronic inflammation using "superfoods". A combination of different foods can work through different pathways to shut down excessive inflammation; nutrition appears to be a key in the fight against chronic inflammation, and the right combination of foods can almost shut down the cytokine storm that overwhelms the patient's body.

In vivo polyphenol administration demonstrated that these nutrients perform well even alone but they can have great potential as an adjuvant to the common anti-inflammatory biologic therapies.

7. Future perspectives

A combinational therapy with more polyphenols in *in vivo* models of chronic inflammation can shed more light on their role and mechanisms to counter excessive inflammation.

Metabolomic and lipidomic analysis of the ileum, colon, and feces of SAMP mice treated with purple corn will provide useful insight into what is modulated at that level by polyphenols.

Administration of a combination of biological drugs (i.e. Infliximab or Anti-IL-1 antibodies) and purple corn or other polyphenols to further boost the anti-inflammatory effects can lead to a potential implementation of a clinical trial protocol.

8. Bibliography

1. Austyn, J.M. Dendritic cells. *Curr. Opin. Hematol.* **1998**, *5*, 3-15.
2. Chen, B.; Zhu, L.; Yang, S.; Su, W. Unraveling the Heterogeneity and Ontogeny of Dendritic Cells Using Single-Cell RNA Sequencing. *Front. Immunol.* **2021**, *12*, 711329.
3. Hemmi, H.; Akira, S. TLR signalling and the function of dendritic cells. *Chem. Immunol. Allergy* **2005**, *86*, 120-135.
4. Krishnaswamy, J.K.; Chu, T.; Eisenbarth, S.C. Beyond pattern recognition: NOD-like receptors in dendritic cells. *Trends Immunol.* **2013**, *34*, 224-233.
5. Théry, C.; Amigorena, S. The cell biology of antigen presentation in dendritic cells. *Curr. Opin. Immunol.* **2001**, *13*, 45-51.
6. Banchereau, J.; Steinman, R.M. Dendritic cells and the control of immunity. *Nature* **1998**, *392*, 245-252.
7. Bernardo, D.; Gisbert, J.P. Human Intestinal Dendritic Cells in Inflammatory Bowel Diseases. *Mol. Nutr. Food Res.* **2018**, *1700931*, 1-8.
8. Waisman, A.; Lukas, D.; Clausen, B.E.; Yogev, N. Dendritic cells as gatekeepers of tolerance. *Semin. Immunopathol.* **2017**, *39*, 153-163.
9. Mellman, I. Dendritic Cells: Master Regulators of the Immune Response. *Cancer Immunology Research* **2013**, *1*, 145-149.
10. Rutella, S.; Locatelli, F. Intestinal dendritic cells in the pathogenesis of inflammatory bowel disease. *World J. Gastroenterol.* **2011**, *17*, 3761-3775.
11. Villani, A.C.; Satija, R.; Reynolds, G.; Sarkizova, S.; Shekhar, K.; Fletcher, J.; Griesbeck, M.; Butler, A.; Zheng, S.; Lazo, S., et al. Single-cell RNA-seq reveals new types of human blood dendritic cells, monocytes, and progenitors. *Science* **2017**, *356*.
12. Hart, A.L.; Al-Hassi, H.O.; Rigby, R.J.; Bell, S.J.; Emmanuel, A.V.; Knight, S.C.; Kamm, M.A.; Stagg, A.J. Characteristics of Intestinal Dendritic Cells in Inflammatory Bowel Diseases. *Gastroenterology* **2005**, *129*, 50-65.
13. Karsunky, H.; Merad, M.; Cozzio, A.; Weissman, I.L.; Manz, M.G. Flt3 ligand regulates dendritic cell development from Flt3+ lymphoid and myeloid-committed progenitors to Flt3+ dendritic cells in vivo. *J. Exp. Med.* **2003**, *198*, 305-313.
14. Chopin, M.; Lun, A.T.; Zhan, Y.; Schreuder, J.; Coughlan, H.; D'Amico, A.; Mielke, L.A.; Almeida, F.F.; Kueh, A.J.; Dickins, R.A., et al. Transcription Factor PU.1 Promotes Conventional Dendritic Cell Identity and Function via Induction of Transcriptional Regulator DC-SCRIPT. *Immunity* **2019**, *50*, 77-90.e75.
15. Merad, M.; Sathe, P.; Helft, J.; Miller, J.; Mortha, A. The dendritic cell lineage: ontogeny and function of dendritic cells and their subsets in the steady state and the inflamed setting. *Annu. Rev. Immunol.* **2013**, *31*, 563-604.

16. Asselin-Paturel, C.; Brizard, G.; Pin, J.J.; Brière, F.; Trinchieri, G. Mouse strain differences in plasmacytoid dendritic cell frequency and function revealed by a novel monoclonal antibody. *J. Immunol.* **2003**, *171*, 6466-6477.
17. Musumeci, A.; Lutz, K.; Winheim, E.; Krug, A.B. What Makes a pDC: Recent Advances in Understanding Plasmacytoid DC Development and Heterogeneity. *Front. Immunol.* **2019**, *10*.
18. Fitzgerald-Bocarsly, P.; Dai, J.; Singh, S. Plasmacytoid dendritic cells and type I IFN: 50 years of convergent history. *Cytokine Growth Factor Rev.* **2008**, *19*, 3-19.
19. Nairz, M.; Theurl, I.; Swirski, F.K.; Weiss, G. "Pumping iron"-how macrophages handle iron at the systemic, microenvironmental, and cellular levels. *Pflugers Archiv : European journal of physiology* **2017**, *469*, 397-418.
20. Knutson, M.D.; Vafa, M.R.; Haile, D.J.; Wessling-resnick, M. Iron loading and erythrophagocytosis increase ferroportin 1 (FPN1) expression in J774 macrophages. *Blood* **2019**, *102*, 4191-4198.
21. Chu, K.-A.; Hsu, C.-H.; Lin, M.-C.; Chu, Y.-H.; Hung, Y.-M.; Wei, J.C.-C. Association of iron deficiency anemia with tuberculosis in Taiwan: A nationwide population-based study. *PLoS One* **2019**, *14*, e0221908.
22. Sottile, R.; Federico, G.; Garofalo, C.; Tallerico, R.; Faniello, M.C.; Quaresima, B.; Cristiani, C.M.; Di Sanzo, M.; Cuda, G.; Ventura, V., et al. Iron and Ferritin Modulate MHC Class I Expression and NK Cell Recognition. *Front. Immunol.* **2019**, *10*, 224.
23. Uz, B. The Effect of Iron Deficiency Anemia Treatment on Neutrophil to Lymphocyte Ratio and Platelet to Lymphocyte Ratio. *Global Journal of Hematology and Blood Transfusion* **2016**, *3*, 1-5.
24. Aly, S.S.; Fayed, H.M.; Ismail, A.M.; Abdel Hakeem, G.L. Assessment of peripheral blood lymphocyte subsets in children with iron deficiency anemia. *BMC Pediatr.* **2018**, *18*, 4-9.
25. Reza Keramati, M.; Sadeghian, M.H.; Ayatollahi, H.; Mahmoudi, M.; Khajedaluea, M.; Tavasolian, H.; Borzouei, A. Peripheral Blood Lymphocyte Subset Counts in Pre-menopausal Women with Iron-Deficiency Anaemia. *The Malaysian journal of medical sciences : MJMS* **2011**, *18*, 38-44.
26. Badr El-Din, N.K.; Noaman, E.; Abdel Fattah, S.M.; Ghoneum, M. Reversal of age-associated oxidative stress in rats by MRN-100, a hydro-ferrate fluid. *In Vivo* **2010**, *24*, 525-533.
27. Ghoneum, M.H.; Badr El-Din, N.K.; Abdel Fattah, S.M.; Pan, D.; Tolentino, L. Hydroferrate fluid, MRN-100, provides protection against chemical-induced gastric and esophageal cancer in wistar rats. *Int. J. Biol. Sci.* **2015**, *11*, 295-303.

28. Ghoneum, M.; Matsuura, M.; Gollapudi, S. An iron-based beverage, HydroFerrate fluid (MRN-100), alleviates oxidative stress in murine lymphocytes in vitro. *Nutr. J.* **2009**, *8*, 1-6.
29. Mazhar, M.; Kabir, N.; Simjee, S.U. Quercetin modulates iron homeostasis and iNOS expression of splenic macrophages in a rat model of iron deficiency anemia. *Chinese journal of natural medicines* **2018**, *16*, 580-589.
30. Hassan, T.H.; Badr, M.A.; Karam, N.A.; Zkaria, M.; El Saadany, H.F.; Rahman, D.M.A.; Shahbah, D.A.; Al Morshedy, S.M.; Fathy, M.; Hosni Esh, A.M., et al. Impact of iron deficiency anemia on the function of the immune system in children. *Medicine (United States)* **2016**, *95*, 1-5.
31. Abbassia Demmouche, S.R. Iron Deficiency Anemia in Children and Alteration of the Immune System. *Journal of Nutrition & Food Sciences* **2014**, *05*, 1-5.
32. Mertens, C.; Akam, E.A.; Rehwald, C.; Brüne, B.; Tomat, E.; Jung, M. Intracellular Iron Chelation Modulates the Macrophage Iron Phenotype with Consequences on Tumor Progression. *PLoS One* **2016**, *11*, e0166164.
33. Özdemir, N. Iron deficiency anemia from diagnosis to treatment in children. *Turk pediatri arsivi* **2015**, *50*, 11-19.
34. Jiang, Y.; Li, C.; Wu, Q.; An, P.; Huang, L.; Wang, J.; Chen, C.; Chen, X.; Zhang, F.; Ma, L., et al. Iron-dependent histone 3 lysine 9 demethylation controls B cell proliferation and humoral immune responses. *Nature Communications* **2019**, *10*.
35. Tolkien, Z.; Stecher, L.; Mander, A.P.; Pereira, D.I.; Powell, J.J. Ferrous sulfate supplementation causes significant gastrointestinal side-effects in adults: a systematic review and meta-analysis. *PLoS One* **2015**, *10*, e0117383.
36. Bosch, X.; Montori, E.; Guerra-García, M.; Costa-Rodríguez, J.; Quintanilla, M.H.; Tolosa-Chapasian, P.E.; Moreno, P.; Guasch, N.; López-Soto, A. Haemoglobin responses to transfusion in severe iron deficiency anaemia: potential impact of gastrointestinal disorders. *Vox Sang.* **2017**, *112*, 257-267.
37. Nixon, C.P.; Sweeney, J.D. Severe iron deficiency anemia: red blood cell transfusion or intravenous iron? *Transfusion* **2018**, *58*, 1824-1826.
38. Ben-Ami, T.; Natour, M.; Rekhtman, D.; Ariel, T.; Revel-Vilk, S. Iron Deficiency Anemia As a Leading Cause of Severe Anemia in Children May be Associated with Unnecessary Red Blood Cells (RBCs) Transfusion. *Blood* **2015**, *126*, 4454.
39. Boone, S.; Powers, J.M.; Goodgame, B.; Peacock, W.F. Identification and Management of Iron Deficiency Anemia in the Emergency Department. *J. Emerg. Med.* **2019**, 10.1016/j.jemermed.2019.08.052, 1-9.
40. Iqbal, T.; Stein, J.; Sharma, N.; Kulnigg-Dabsch, S.; Vel, S.; Gasche, C. Clinical significance of C-reactive protein levels in predicting responsiveness

to iron therapy in patients with inflammatory bowel disease and iron deficiency anemia. *Dig. Dis. Sci.* **2015**, *60*, 1375-1381.
41. Lichtenstein, G.R.; Onken, J.E. Improved Hemoglobin Response with Ferric Carboxymaltose in Patients with Gastrointestinal-Related Iron-Deficiency Anemia Versus Oral Iron. *Dig. Dis. Sci.* **2018**, *63*, 3009-3019.
42. Fraga, C.G.; Croft, K.D.; Kennedy, D.O.; Tomás-Barberán, F.A. The effects of polyphenols and other bioactives on human health. *Food Funct.* **2019**, *10*, 514-528.
43. Galleggiante, V.; De Santis, S.; Cavalcanti, E.; Scarano, A.; De Benedictis, M.; Serino, G.; Caruso, M.L.; Mastronardi, M.; Pinto, A.; Campiglia, P., et al. Dendritic Cells Modulate Iron Homeostasis and Inflammatory Abilities Following Quercetin Exposure. *Curr. Pharm. Des.* **2017**, *23*, 2139-2146.
44. Cavalcanti, E.; Vadrucci, E.; Delvecchio, F.R.; Addabbo, F.; Bettini, S.; Liou, R.; Monsurrò, V.; Huang, A.Y.C.; Pizarro, T.T.; Santino, A., et al. Administration of reconstituted polyphenol oil bodies efficiently suppresses dendritic cell inflammatory pathways and acute intestinal inflammation. *PLoS One* **2014**, *9*.
45. De Santis, S.; Kunde, D.; Serino, G.; Galleggiante, V.; Caruso, M.L.; Mastronardi, M.; Cavalcanti, E.; Ranson, N.; Pinto, A.; Campiglia, P., et al. Secretory leukoprotease inhibitor is required for efficient quercetin-mediated suppression of TNFβ secretion. *Oncotarget* **2016**, *7*, 75800-75809.
46. Adesso, S.; Pepe, G.; Sommella, E.; Manfra, M.; Scopa, A.; Sofo, A.; Tenore, G.C.; Russo, M.; Di Gaudio, F.; Autore, G., et al. Anti-inflammatory and antioxidant activity of polyphenolic extracts from Lactuca sativa (var. Maravilla de Verano) under different farming methods. *J. Sci. Food Agric.* **2016**, *96*, 4194-4206.
47. Pepe, G.; Pagano, F.; Adesso, S.; Sommella, E.; Ostacolo, C.; Manfra, M.; Chieppa, M.; Sala, M.; Russo, M.; Marzocco, S., et al. Bioavailable Citrus sinensis Extract: Polyphenolic Composition and Biological Activity. *Molecules (Basel, Switzerland)* **2017**, *22*, 623.
48. Pepe, G.; Sommella, E.; Cianciarulo, D.; Ostacolo, C.; Manfra, M.; Di Sarno, V.; Musella, S.; Russo, M.; Messore, A.; Parrino, B., et al. Polyphenolic Extract from Tarocco (Citrus sinensis L. Osbeck) Clone "Lempso" Exerts Anti-Inflammatory and Antioxidant Effects via NF-kB and Nrf-2 Activation in Murine Macrophages. *Nutrients* **2018**, *10*, 1961.
49. Procaccini, C.; Galgani, M.; De Rosa, V.; Matarese, G. Intracellular metabolic pathways control immune tolerance. *Trends Immunol.* **2012**, *33*, 1-7.
50. Sommella, E.; Verna, G.; Liso, M.; Salviati, E.; Esposito, T.; Carbone, D.; Pecoraro, C.; Chieppa, M.; Campiglia, P. Hop-derived fraction rich in beta acids and prenylflavonoids regulates the inflammatory response in dendritic

cells differently from quercetin: unveiling metabolic changes by mass spectrometry-based metabolomics. *Food Funct.* **2021**, *12*, 12800-12811.
51. Brissot, P.; Ropert, M.; Le Lan, C.; Loréal, O. Non-transferrin bound iron: A key role in iron overload and iron toxicity. *Biochimica et Biophysica Acta (BBA) - General Subjects* **2012**, *1820*, 403-410.
52. Mohammad, A.A. Myelodysplastic syndrome from theoretical review to clinical application view. *Oncol. Rev.* **2018**, *12*, 134-142.
53. Gao, C.; Li, L.; Chen, B.; Song, H.; Cheng, J.; Zhang, X.; Sun, Y. Clinical outcomes of transfusion-associated iron overload in patients with refractory chronic anemia. *Patient preference and adherence* **2014**, *8*, 513-517.
54. Chai, X.; Li, D.; Cao, X.; Zhang, Y.; Mu, J.; Lu, W.; Xiao, X.; Li, C.; Meng, J.; Chen, J., et al. ROS-mediated iron overload injures the hematopoiesis of bone marrow by damaging hematopoietic stem/progenitor cells in mice. *Sci. Rep.* **2015**, *5*, 1-12.
55. Zeidan, A.M.; Pullarkat, V.A.; Komrokji, R.S. Overcoming barriers to treating iron overload in patients with lower-risk myelodysplastic syndrome. *Crit. Rev. Oncol. Hematol.* **2017**, *117*, 57-66.
56. Wong, C.A.C.; Wong, S.A.Y.; Leitch, H.A. Iron overload in lower international prognostic scoring system risk patients with myelodysplastic syndrome receiving red blood cell transfusions: Relation to infections and possible benefit of iron chelation therapy. *Leuk. Res.* **2018**, *67*, 75-81.
57. Jin, X.; He, X.; Cao, X.; Xu, P.; Xing, Y.; Sui, S.; Wang, L.; Meng, J.; Lu, W.; Cui, R., et al. Iron overload impairs normal hematopoietic stem and progenitor cells through reactive oxygen species and shortens survival in myelodysplastic syndrome mice. *Haematologica* **2018**, *103*, 1627-1634.
58. De Santis, S.; Galleggiante, V.; Scandiffio, L.; Liso, M.; Sommella, E.; Sobolewski, A.; Spilotro, V.; Pinto, A.; Campiglia, P.; Serino, G., et al. Secretory Leukoprotease Inhibitor (Slpi) Expression Is Required for Educating Murine Dendritic Cells Inflammatory Response Following Quercetin Exposure. *Nutrients* **2017**, *9*, 706.
59. Delvecchio, F.R.; Vadrucci, E.; Cavalcanti, E.; De Santis, S.; Kunde, D.; Vacca, M.; Myers, J.; Allen, F.; Bianco, G.; Huang, A.Y., et al. Polyphenol administration impairs T-cell proliferation by imprinting a distinct dendritic cell maturational profile. *Eur. J. Immunol.* **2015**, *45*, 2638-2649.
60. Dicarlo, M.; Teti, G.; Verna, G.; Liso, M.; Cavalcanti, E.; Sila, A.; Raveenthiraraj, S.; Mastronardi, M.; Santino, A.; Serino, G., et al. Quercetin Exposure Suppresses the Inflammatory Pathway in Intestinal Organoids from Winnie Mice. *Int. J. Mol. Sci.* **2019**, *20*.
61. Verna, G.; Liso, M.; Cavalcanti, E.; Bianco, G.; Di Sarno, V.; Santino, A.; Campiglia, P.; Chieppa, M. Quercetin Administration Suppresses the Cytokine Storm in Myeloid and Plasmacytoid Dendritic Cells. *Int. J. Mol. Sci.* **2021**, *22*, 8349.

62. Cariello, M.; Contursi, A.; Gadaleta, R.M.; Piccinin, E.; De Santis, S.; Piglionica, M.; Spaziante, A.F.; Sabbà, C.; Villani, G.; Moschetta, A. Extra-Virgin Olive Oil from Apulian Cultivars and Intestinal Inflammation. *Nutrients* **2020**, *12*.
63. De Santis, S.; Liso, M.; Verna, G.; Curci, F.; Milani, G.; Faienza, M.F.; Franchini, C.; Moschetta, A.; Chieppa, M.; Clodoveo, M.L., et al. Extra Virgin Olive Oil Extracts Modulate the Inflammatory Ability of Murine Dendritic Cells Based on Their Polyphenols Pattern: Correlation between Chemical Composition and Biological Function. *Antioxidants (Basel, Switzerland)* **2021**, *10*.
64. De Santis, S.; Cariello, M.; Piccinin, E.; Sabbà, C.; Moschetta, A. Extra Virgin Olive Oil: Lesson from Nutrigenomics. *Nutrients* **2019**, *11*.
65. Eri, R.D.; Adams, R.J.; Tran, T.V.; Tong, H.; Das, I.; Roche, D.K.; Oancea, I.; Png, C.W.; Jeffery, P.L.; Radford-Smith, G.L., et al. An intestinal epithelial defect conferring ER stress results in inflammation involving both innate and adaptive immunity. *Mucosal Immunol.* **2011**, *4*, 354-364.
66. Liso, M.; De Santis, S.; Scarano, A.; Verna, G.; Dicarlo, M.; Galleggiante, V.; Campiglia, P.; Mastronardi, M.; Lippolis, A.; Vacca, M., et al. A Bronze-Tomato Enriched Diet Affects the Intestinal Microbiome under Homeostatic and Inflammatory Conditions. *Nutrients* **2018**, *10*.
67. Scarano, A.; Butelli, E.; De Santis, S.; Cavalcanti, E.; Hill, L.; De Angelis, M.; Giovinazzo, G.; Chieppa, M.; Martin, C.; Santino, A. Combined Dietary Anthocyanins, Flavonols, and Stilbenoids Alleviate Inflammatory Bowel Disease Symptoms in Mice. *Front Nutr* **2018**, *4*, 75-75.
68. De Santis, S.; Scarano, A.; Liso, M.; Calabrese, F.M.; Verna, G.; Cavalcanti, E.; Sila, A.; Lippolis, A.; De Angelis, M.; Santino, A., et al. Polyphenol Enriched Diet Administration During Pregnancy and Lactation Prevents Dysbiosis in Ulcerative Colitis Predisposed Littermates. *Frontiers in Cellular and Infection Microbiology* **2021**, *11*, 456.
69. Scarano, A.; Chieppa, M.; Santino, A. Plant Polyphenols-Biofortified Foods as a Novel Tool for the Prevention of Human Gut Diseases. *Antioxidants (Basel, Switzerland)* **2020**, *9*, 1225.
70. Corridoni, D.; Arseneau, K.O.; Cominelli, F. Inflammatory bowel disease. *Immunol. Lett.* **2014**, *161*, 231-235.
71. Roda, G.; Chien Ng, S.; Kotze, P.G.; Argollo, M.; Panaccione, R.; Spinelli, A.; Kaser, A.; Peyrin-Biroulet, L.; Danese, S. Crohn's disease. *Nature Reviews Disease Primers* **2020**, *6*, 22.
72. Khalili, H.; Håkansson, N.; Chan, S.S.; Chen, Y.; Lochhead, P.; Ludvigsson, J.F.; Chan, A.T.; Hart, A.R.; Olén, O.; Wolk, A. Adherence to a Mediterranean diet is associated with a lower risk of later-onset Crohn's disease: results from two large prospective cohort studies. *Gut* **2020**, *69*, 1637-1644.

73. Huang, H.; Fang, M.; Jostins, L.; Umićević Mirkov, M.; Boucher, G.; Anderson, C.A.; Andersen, V.; Cleynen, I.; Cortes, A.; Crins, F., et al. Fine-mapping inflammatory bowel disease loci to single-variant resolution. *Nature* **2017**, *547*, 173-178.
74. Uhlig, H.H.; Powrie, F. Translating Immunology into Therapeutic Concepts for Inflammatory Bowel Disease. *Annu. Rev. Immunol.* **2018**, *36*, 755-781.
75. Feagan, B.G.; Rutgeerts, P.; Sands, B.E.; Hanauer, S.; Colombel, J.-F.; Sandborn, W.J.; Van Assche, G.; Axler, J.; Kim, H.-J.; Danese, S., et al. Vedolizumab as Induction and Maintenance Therapy for Ulcerative Colitis. *N. Engl. J. Med.* **2013**, *369*, 699-710.
76. Feagan, B.G.; Sandborn, W.J.; Gasink, C.; Jacobstein, D.; Lang, Y.; Friedman, J.R.; Blank, M.A.; Johanns, J.; Gao, L.-L.; Miao, Y., et al. Ustekinumab as Induction and Maintenance Therapy for Crohn's Disease. *N. Engl. J. Med.* **2016**, *375*, 1946-1960.
77. Dulai, P.S.; Singh, S.; Jiang, X.; Peerani, F.; Narula, N.; Chaudrey, K.; Whitehead, D.; Hudesman, D.; Lukin, D.; Swaminath, A., et al. The Real-World Effectiveness and Safety of Vedolizumab for Moderate-Severe Crohn's Disease: Results From the US VICTORY Consortium. *Am. J. Gastroenterol.* **2016**, *111*, 1147-1155.
78. Nieminen, J.K.; Niemi, M.; Sipponen, T.; Salo, H.M.; Klemetti, P.; Färkkilä, M.; Vakkila, J.; Vaarala, O. Dendritic Cells from Crohn's Disease Patients Show Aberrant STAT1 and STAT3 Signaling. *PLoS One* **2013**, *8*, e70738.
79. Cooney, R.; Baker, J.; Brain, O.; Danis, B.; Pichulik, T.; Allan, P.; Ferguson, D.J.P.; Campbell, B.J.; Jewell, D.; Simmons, A. NOD2 stimulation induces autophagy in dendritic cells influencing bacterial handling and antigen presentation. *Nat. Med.* **2010**, *16*, 90-97.
80. van Beelen, A.J.; Zelinkova, Z.; Taanman-Kueter, E.W.; Muller, F.J.; Hommes, D.W.; Zaat, S.A.J.; Kapsenberg, M.L.; de Jong, E.C. Stimulation of the Intracellular Bacterial Sensor NOD2 Programs Dendritic Cells to Promote Interleukin-17 Production in Human Memory T Cells. *Immunity* **2007**, *27*, 660-669.
81. Liu, H.; Chen, F.; Wu, W.; Cao, A.T.; Xue, X.; Yao, S.; Evans-Marin, H.L.; Li, Y.-Q.; Cong, Y. TLR5 mediates CD172α+ intestinal lamina propria dendritic cell induction of Th17 cells. *Sci. Rep.* **2016**, *6*, 22040.
82. Kinnebrew, Melissa A.; Buffie, Charlie G.; Diehl, Gretchen E.; Zenewicz, Lauren A.; Leiner, I.; Hohl, Tobias M.; Flavell, Richard A.; Littman, Dan R.; Pamer, Eric G. Interleukin 23 Production by Intestinal CD103+CD11b+ Dendritic Cells in Response to Bacterial Flagellin Enhances Mucosal Innate Immune Defense. *Immunity* **2012**, *36*, 276-287.
83. Ng, S.C.; Benjamin, J.L.; McCarthy, N.E.; Hedin, C.R.H.; Koutsoumpas, A.; Plamondon, S.; Price, C.L.; Hart, A.L.; Kamm, M.A.; Forbes, A., et al. Relationship between human intestinal dendritic cells, gut microbiota, and

disease activity in Crohn's disease. *Inflamm. Bowel Dis.* **2010**, *17*, 2027-2037.
84. Stagg, A.J. Intestinal Dendritic Cells in Health and Gut Inflammation. *Front. Immunol.* **2018**, *9*.
85. Johansson-Lindbom, B.; Svensson, M.; Pabst, O.; Palmqvist, C.; Marquez, G.; Förster, R.; Agace, W.W. Functional specialization of gut CD103+ dendritic cells in the regulation of tissue-selective T cell homing. *J. Exp. Med.* **2005**, *202*, 1063-1073.
86. Scott, C.L.; Aumeunier, A.M.; Mowat, A.M. Intestinal CD103+ dendritic cells: master regulators of tolerance? *Trends Immunol.* **2011**, *32*, 412-419.
87. Bates, J.; Diehl, L. Dendritic cells in IBD pathogenesis: an area of therapeutic opportunity? *J. Pathol.* **2014**, *232*, 112-120.
88. Pizarro, T.T.; Pastorelli, L.; Bamias, G.; Garg, R.R.; Reuter, B.K.; Mercado, J.R.; Chieppa, M.; Arseneau, K.O.; Ley, K.; Cominelli, F. SAMP1/YitFc mouse strain: A spontaneous model of Crohn's disease-like ileitis. *Inflamm. Bowel Dis.* **2010**, *17*, 2566-2584.
89. De Salvo, C.; Buela, K.A.; Creyns, B.; Corridoni, D.; Rana, N.; Wargo, H.L.; Cominelli, C.L.; Delaney, P.G.; Rodriguez-Palacios, A.; Cominelli, F., et al. NOD2 drives early IL-33-dependent expansion of group 2 innate lymphoid cells during Crohn's disease-like ileitis. *J. Clin. Invest.* **2021**, *131*.
90. Corridoni, D.; Kodani, T.; Rodriguez-Palacios, A.; Pizarro, T.T.; Xin, W.; Nickerson, K.P.; McDonald, C.; Ley, K.F.; Abbott, D.W.; Cominelli, F. Dysregulated NOD2 predisposes SAMP1/YitFc mice to chronic intestinal inflammation. *Proceedings of the National Academy of Sciences* **2013**, *110*, 16999-17004.
91. Mikulski, Z.; Johnson, R.; Shaked, I.; Kim, G.; Nowyhed, H.; Goodman, W.; Chodaczek, G.; Pizarro, T.T.; Cominelli, F.; Ley, K. SAMP1/YitFc Mice Develop Ileitis via Loss of CCL21 and Defects in Dendritic Cell Migration. *Gastroenterology* **2015**, *148*, 783-793.e785.
92. Matheu, M.P.; Sen, D.; Cahalan, M.D.; Parker, I. Generation of bone marrow derived murine dendritic cells for use in 2-photon imaging. *Journal of visualized experiments : JoVE* **2008**, 10.3791/773.
93. Wang, W.; Li, J.; Wu, K.; Azhati, B.; Rexiati, M. Culture and Identification of Mouse Bone Marrow-Derived Dendritic Cells and Their Capability to Induce T Lymphocyte Proliferation. *Med. Sci. Monit.* **2016**, *22*, 244-250.
94. Xu, Y.; Zhan, Y.; Lew, A.M.; Naik, S.H.; Kershaw, M.H. Differential Development of Murine Dendritic Cells by GM-CSF versus Flt3 Ligand Has Implications for Inflammation and Trafficking. *The Journal of Immunology* **2007**, *179*, 7577.
95. Salviati, E.; Ciaglia, E.; Sommella, E.; Montella, F.; Bertamino, A.; Ostacolo, C.; Parrino, B.; Rubino, R.; Vecchione, C.; Puca, A., et al. Immunomodulatory activity of Humulus lupulus bitter acids fraction:

Enhancement of natural killer cells function by NKp44 activating receptor stimulation. *J. Funct. Foods* **2019**, *61*, 103469.
96. Magni, G.; Marinelli, A.; Riccio, D.; Lecca, D.; Tonelli, C.; Abbracchio, M.P.; Petroni, K.; Ceruti, S. Purple Corn Extract as Anti-allodynic Treatment for Trigeminal Pain: Role of Microglia. *Front. Cell. Neurosci.* **2018**, *12*, 378.
97. Petroni, K.; Trinei, M.; Fornari, M.; Calvenzani, V.; Marinelli, A.; Micheli, L.A.; Pilu, R.; Matros, A.; Mock, H.P.; Tonelli, C., et al. Dietary cyanidin 3-glucoside from purple corn ameliorates doxorubicin-induced cardiotoxicity in mice. *Nutr. Metab. Cardiovasc. Dis.* **2017**, *27*, 462-469.
98. Shannon, C.E. The mathematical theory of communication. 1963. *MD Comput.* **1997**, *14*, 306-317.
99. Chao, A.; Bunge, J. Estimating the number of species in a stochastic abundance model. *Biometrics* **2002**, *58*, 531-539.
100. Cooper, A.M.; Khader, S.A. IL-12p40: an inherently agonistic cytokine. *Trends Immunol.* **2007**, *28*, 33-38.
101. Dinarello, C.A. Overview of the IL-1 family in innate inflammation and acquired immunity. *Immunol. Rev.* **2018**, *281*, 8-27.
102. Haschka, D.; Petzer, V.; Kocher, F.; Tschurtschenthaler, C.; Schaefer, B.; Seifert, M.; Sopper, S.; Sonnweber, T.; Feistritzer, C.; Arvedson, T.L., et al. Classical and intermediate monocytes scavenge non-transferrin-bound iron and damaged erythrocytes. *JCI insight* **2019**, *4*, e98867.
103. Sukhbaatar, N.; Weichhart, T. Iron Regulation: Macrophages in Control. *Pharmaceuticals (Basel)* **2018**, *11*, 137.
104. Lee, J.; Zhou, Y.J.; Ma, W.; Zhang, W.; Aljoufi, A.; Luh, T.; Lucero, K.; Liang, D.; Thomsen, M.; Bhagat, G., et al. Lineage specification of human dendritic cells is marked by IRF8 expression in hematopoietic stem cells and multipotent progenitors. *Nat. Immunol.* **2017**, *18*, 877-888.
105. Kaisho, T.; Akira, S. Dendritic-cell function in Toll-like receptor- and MyD88-knockout mice. *Trends Immunol.* **2001**, *22*, 78-83.
106. Mazgaeen, L.; Gurung, P. Recent Advances in Lipopolysaccharide Recognition Systems. *Int. J. Mol. Sci.* **2020**, *21*.
107. Tait Wojno, E.D.; Hunter, C.A.; Stumhofer, J.S. The Immunobiology of the Interleukin-12 Family: Room for Discovery. *Immunity* **2019**, *50*, 851-870.
108. Parks, O.B.; Pociask, D.A.; Hodzic, Z.; Kolls, J.K.; Good, M. Interleukin-22 Signaling in the Regulation of Intestinal Health and Disease. *Frontiers in Cellular and Developmental Biology* **2016**, *3*.
109. Richez, C.; Yasuda, K.; Watkins, A.A.; Akira, S.; Lafyatis, R.; van Seventer, J.M.; Rifkin, I.R. TLR4 Ligands Induce IFN-α Production by Mouse Conventional Dendritic Cells and Human Monocytes after IFN-β Priming. *The Journal of Immunology* **2009**, *182*, 820-828.

110. Okada, T.; Lian, Z.-X.; Naiki, M.; Ansari, A.A.; Ikehara, S.; Gershwin, M.E. Murine thymic plasmacytoid dendritic cells. *Eur. J. Immunol.* **2003**, *33*, 1012-1019.
111. Egea, L.; Hirata, Y.; Kagnoff, M.F. GM-CSF: a role in immune and inflammatory reactions in the intestine. *Expert Rev. Gastroenterol. Hepatol.* **2010**, *4*, 723-731.
112. Lonial, S.; Akhtari, M.; Kaufman, J.; Torre, C.; Lechowicz, M.J.; Flowers, C.; Sinha, R.; Khoury, H.J.; Langston, A.A.; Waller, E.K. Mobilization of Hematopoietic Progenitors from Normal Donors Using the Combination of Granulocyte-Macrophage Colony-Stimulating Factor and Granulocyte Colony-Stimulating Factor Results in Fewer Plasmacytoid Dendritic Cells in the Graft and Enhanced Donor T Cell Engraftment with Th1 Polarization: Results from a Randomized Clinical Trial. *Biol. Blood Marrow Transplant.* **2013**, *19*, 460-467.
113. Roberts, A.W. G-CSF: a key regulator of neutrophil production, but that's not all! *Growth Factors* **2005**, *23*, 33-41.
114. Sesti-Costa, R.; Cervantes-Barragan, L.; Swiecki, M.K.; Fachi, J.L.; Cella, M.; Gilfillan, S.; Silva, J.S.; Colonna, M. Leukemia Inhibitory Factor Inhibits Plasmacytoid Dendritic Cell Function and Development. *The Journal of Immunology* **2020**, *204*, 2257-2268.
115. Na, Y.R.; Jung, D.; Stakenborg, M.; Jang, H.; Gu, G.J.; Jeong, M.R.; Suh, S.Y.; Kim, H.J.; Kwon, Y.H.; Sung, T.S., et al. Prostaglandin E(2) receptor PTGER4-expressing macrophages promote intestinal epithelial barrier regeneration upon inflammation. *Gut* **2021**, 10.1136/gutjnl-2020-322146.
116. Birmachu, W.; Gleason, R.M.; Bulbulian, B.J.; Riter, C.L.; Vasilakos, J.P.; Lipson, K.E.; Nikolsky, Y. Transcriptional networks in plasmacytoid dendritic cells stimulated with synthetic TLR 7 agonists. *BMC Immunol.* **2007**, *8*, 26.
117. Kriehuber, E.; Bauer, W.; Charbonnier, A.-S.; Winter, D.; Amatschek, S.; Tamandl, D.; Schweifer, N.; Stingl, G.; Maurer, D. Balance between NF-κB and JNK/AP-1 activity controls dendritic cell life and death. *Blood* **2005**, *106*, 175-183.
118. Sun, G.; Chen, Z.; Jasmer, K.; Chuang, D.; Gu, Z.; Hannink, M.; Simonyi, A. Quercetin Attenuates Inflammatory Responses in BV-2 Microglial Cells: Role of MAPKs on the Nrf2 Pathway and Induction of Heme Oxygenase-1. *PLoS One* **2015**, *10*, e0141509.
119. Yamamoto, Y.; Yamasuge, W.; Imai, S.; Kunisawa, K.; Hoshi, M.; Fujigaki, H.; Mouri, A.; Nabeshima, T.; Saito, K. Lipopolysaccharide shock reveals the immune function of indoleamine 2,3-dioxygenase 2 through the regulation of IL-6/stat3 signalling. *Sci. Rep.* **2018**, *8*, 15917.

120. Prendergast, G.C.; Metz, R.; Muller, A.J.; Merlo, L.M.F.; Mandik-Nayak, L. IDO2 in Immunomodulation and Autoimmune Disease. *Front. Immunol.* **2014**, *5*.
121. Weber, N.; Biehler, K.; Schwabe, K.; Haarhaus, B.; Quirin, K.-W.; Frank, U.; Schempp, C.M.; Wölfle, U. Hop Extract Acts as an Antioxidant with Antimicrobial Effects against Propionibacterium Acnes and Staphylococcus Aureus. *Molecules (Basel, Switzerland)* **2019**, *24*, 223.
122. Bland, J.S.; Minich, D.; Lerman, R.; Darland, G.; Lamb, J.; Tripp, M.; Grayson, N. Isohumulones from hops (Humulus lupulus) and their potential role in medical nutrition therapy. *PharmaNutrition* **2015**, *3*, 46-52.
123. Hayes, J.D.; Dinkova-Kostova, A.T. The Nrf2 regulatory network provides an interface between redox and intermediary metabolism. *Trends Biochem. Sci.* **2014**, *39*, 199-218.
124. Kelly, B.; O'Neill, L.A.J. Metabolic reprogramming in macrophages and dendritic cells in innate immunity. *Cell Res.* **2015**, *25*, 771-784.
125. Wculek, S.; Khouili, S.; Priego, E.; Heras-Murillo, I.; Sancho, D. Metabolic Control of Dendritic Cell Functions: Digesting Information. *Front. Immunol.* **2019**, *10*, 775.
126. He, F.; Ru, X.; Wen, T. NRF2, a Transcription Factor for Stress Response and Beyond. *Int. J. Mol. Sci.* **2020**, *21*, 4777.
127. Holmström, K.M.; Baird, L.; Zhang, Y.; Hargreaves, I.; Chalasani, A.; Land, J.M.; Stanyer, L.; Yamamoto, M.; Dinkova-Kostova, A.T.; Abramov, A.Y. Nrf2 impacts cellular bioenergetics by controlling substrate availability for mitochondrial respiration. *Biol Open* **2013**, *2*, 761-770.
128. Kimura, A.; Kitajima, M.; Nishida, K.; Serada, S.; Fujimoto, M.; Naka, T.; Fujii-Kuriyama, Y.; Sakamato, S.; Ito, T.; Handa, H., et al. NQO1 inhibits the TLR-dependent production of selective cytokines by promoting IκB-ζ degradation. *J. Exp. Med.* **2018**, *215*, 2197-2209.
129. Zolotukhin, P.; Belanova, A. Feed-Forward and Feed-Back Circuits of the NRF2/AP-1 Composite Pathway. In *A Master Regulator of Oxidative Stress - The Transcription Factor Nrf2*, Morales-Gonzalez, J.A., Ed. 2016; 10.5772/65216.
130. Krawczyk, C.M.; Holowka, T.; Sun, J.; Blagih, J.; Amiel, E.; DeBerardinis, R.J.; Cross, J.R.; Jung, E.; Thompson, C.B.; Jones, R.G., et al. Toll-like receptor–induced changes in glycolytic metabolism regulate dendritic cell activation. *Blood* **2010**, *115*, 4742-4749.
131. Rattigan, K.M.; Pountain, A.W.; Regnault, C.; Achcar, F.; Vincent, I.M.; Goodyear, C.S.; Barrett, M.P. Metabolomic profiling of macrophages determines the discrete metabolomic signature and metabolomic interactome triggered by polarising immune stimuli. *PLoS One* **2018**, *13*, e0194126.

132. Ma, J.; Wei, K.; Liu, J.; Tang, K.; Zhang, H.; Zhu, L.; Chen, J.; Li, F.; Xu, P.; Chen, J., et al. Glycogen metabolism regulates macrophage-mediated acute inflammatory responses. *Nature Communications* **2020**, *11*, 1769.
133. McKay, T.B.; Sarker-Nag, A.; Lyon, D.; Asara, J.M.; Karamichos, D. Quercetin modulates keratoconus metabolism in vitro. *Cell Biochem. Funct.* **2015**, *33*, 341-350.
134. Pålsson-McDermott, E.M.; O'Neill, L.A.J. Targeting immunometabolism as an anti-inflammatory strategy. *Cell Res.* **2020**, *30*, 300-314.
135. Ghashghaeinia, M.; Giustarini, D.; Koralkova, P.; Köberle, M.; Alzoubi, K.; Bissinger, R.; Hosseinzadeh, Z.; Dreischer, P.; Bernhardt, I.; Lang, F., et al. Pharmacological targeting of glucose-6-phosphate dehydrogenase in human erythrocytes by Bay 11–7082, parthenolide and dimethyl fumarate. *Sci. Rep.* **2016**, *6*, 28754.
136. Liu, X.; Zhou, W.; Zhang, X.; Lu, P.; Du, Q.; Tao, L.; Ding, Y.; Wang, Y.; Hu, R. Dimethyl fumarate ameliorates dextran sulfate sodium-induced murine experimental colitis by activating Nrf2 and suppressing NLRP3 inflammasome activation. *Biochem. Pharmacol.* **2016**, *112*, 37-49.
137. Tannahill, G.M.; Curtis, A.M.; Adamik, J.; Palsson-McDermott, E.M.; McGettrick, A.F.; Goel, G.; Frezza, C.; Bernard, N.J.; Kelly, B.; Foley, N.H., et al. Succinate is an inflammatory signal that induces IL-1β through HIF-1α. *Nature* **2013**, *496*, 238-242.
138. Liso, M.; Sila, A.; Verna, G.; Scarano, A.; Donghia, R.; Castellana, F.; Cavalcanti, E.; Pesole, P.L.; Sommella, E.M.; Lippolis, A., et al. Nutritional Regimes Enriched with Antioxidants as an Efficient Adjuvant for IBD Patients under Infliximab Administration, a Pilot Study. *Antioxidants (Basel, Switzerland)* **2022**, *11*.
139. McNamee, E.N.; Rivera-Nieves, J. Ectopic Tertiary Lymphoid Tissue in Inflammatory Bowel Disease: Protective or Provocateur? *Front. Immunol.* **2016**, *7*.
140. Rodríguez-Daza, M.C.; Pulido-Mateos, E.C.; Lupien-Meilleur, J.; Guyonnet, D.; Desjardins, Y.; Roy, D. Polyphenol-Mediated Gut Microbiota Modulation: Toward Prebiotics and Further. *Front Nutr* **2021**, *8*.
141. Plamada, D.; Vodnar, D.C. Polyphenols-Gut Microbiota Interrelationship: A Transition to a New Generation of Prebiotics. *Nutrients* **2021**, *14*.
142. Ephraim, E.; Brockman, J.A.; Jewell, D.E. A Diet Supplemented with Polyphenols, Prebiotics and Omega-3 Fatty Acids Modulates the Intestinal Microbiota and Improves the Profile of Metabolites Linked with Anxiety in Dogs. *Biology* **2022**, *11*.
143. Lei, Y.; Tang, L.; Liu, S.; Hu, S.; Wu, L.; Liu, Y.; Yang, M.; Huang, S.; Tang, X.; Tang, T., et al. Parabacteroides produces acetate to alleviate heparanase-exacerbated acute pancreatitis through reducing neutrophil infiltration. *Microbiome* **2021**, *9*, 115.

144. Cladis, D.P.; Simpson, A.M.R.; Cooper, K.J.; Nakatsu, C.H.; Ferruzzi, M.G.; Weaver, C.M. Blueberry polyphenols alter gut microbiota & phenolic metabolism in rats. *Food Funct.* **2021**, *12*, 2442-2456.
145. Butera, A.; Di Paola, M.; Pavarini, L.; Strati, F.; Pindo, M.; Sanchez, M.; Cavalieri, D.; Boirivant, M.; De Filippo, C. Nod2 Deficiency in mice is Associated with Microbiota Variation Favouring the Expansion of mucosal CD4+ LAP+ Regulatory Cells. *Sci. Rep.* **2018**, *8*, 14241.
146. Liso, M.; De Santis, S.; Verna, G.; Dicarlo, M.; Calasso, M.; Santino, A.; Gigante, I.; Eri, R.; Raveenthiraraj, S.; Sobolewski, A., et al. A Specific Mutation in Muc2 Determines Early Dysbiosis in Colitis-Prone Winnie Mice. *Inflamm. Bowel Dis.* **2020**, *26*, 546-556.
147. Verediano, T.A.; Stampini Duarte Martino, H.; Dias Paes, M.C.; Tako, E. Effects of Anthocyanin on Intestinal Health: A Systematic Review. *Nutrients* **2021**, *13*.
148. Komatsu, Y.; Shimizu, Y.; Yamano, M.; Kikuchi, M.; Nakamura, K.; Ayabe, T.; Aizawa, T. Disease progression-associated alterations in fecal metabolites in SAMP1/YitFc mice, a Crohn's disease model. *Metabolomics* **2020**, *16*, 48.